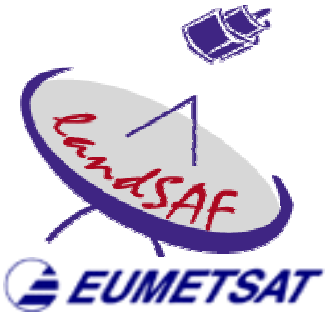

VISITING SCIENTIST REPORT

Evaluation of the DISMA prototyping algorithm for vegetation parameters retrieval on a global scale using the BRDF POLDER/ADEOS database

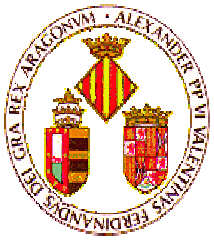

VISITING SCIENTIST: **Fernando Camacho de Coca**

ORGANISATION: **Universitat de València** (1)

PLACE: **MEDIAS-FRANCE** (2) **(Toulouse)**

SUPERVISOR: **Dr. Marc Leroy**

TIME: **February-April 2003 (3 months)**

(1)-Unitat d'Investigació de Teledetecció. Departament de Termodinàmica. Universitat de València. C/ Dr. Moliner, 50. 46100. Burjassot, Valencia, España.

(2)- MEDIAS-FRANCE, Group d'intérêt public, CNES/Météo-France/IRD/CNRS-INSU/UPS/CLS/SPOT-IMAGE. CNES, 18, avenue Edouard Belin, BPI 2102, 31401. Toulouse Cedex 4, France.

CONTENTS

SUMMARY

Our concern in LSA SAF is to develop an operational algorithm for retrieving fractional vegetation cover (FVC) and leaf area index (LAI) on a global scale using spectral and directional information provided by MSG and EPS data. The overall prototype consists of two inversion approaches: (1) The VMESMA procedure, which is an optimised spectral mixture analysis, applied on a variable base using the nadir-zenith (k_0) as input data for the inversion. The output of the VMESMA is the FVC. The LAI is obtained using a semi-empirical relationship. The VMESMA outputs will serve as backup for the more sophisticated DISMA algorithm, assuring the FVC/LAI product also if only spectral information is available (e.g. poor directional sampling to invert satisfactorily DISMA model). Furthermore, the FVC derived with VMESMA will serve as prior information in order to define more accurately the admitted solutions in the inversion of the DISMA model. In addition, the statistical analysis of the images during the execution of VMESMA will also serve to define properly some inputs of the DISMA, in particular, the soil spectral contribution and leaf albedo. (2) The DISMA algorithm, which relies on a physical model inversion, applied also on a variable base using the spectral and directional information, to retrieve simultaneously FVC and LAI

The purpose of this visiting scientist stage has been to evaluate the physical functionality and performance of the DISMA algorithm (see section 2) by prototyping with POLDER/ADEOS BRDF monthly synthesis database. For that, some inputs of the model, such us the soil BRDF model or the clumping index, have been defined (see section 3). In addition, an automatic method to retrieve leaf albedo from the data has been tested providing good results.

The feasibility of the algorithm has been evaluated against POLDER vegetation products, which have been obtained using empirical relationships with vegetation indices and physical model inversion approaches. The results (see section 4) confirm that the DISMA prototype provide reasonable estimates for the full range of variation of FVC and LAI for biomes of very different architecture. These results from the prototyping have constituted a valuable means of testing the underlying physics of the algorithm and also for improving some parts of the DISMA algorithm.

1.INTRODUCTION

Satellite Application Facilities (SAF) on Land Surface Analysis (LSA) is aimed to produce and disseminate geophysical parameters from the synergistic use of the geostationary Meteosat Second Generation (MSG) and polar orbiting European Polar System (EPS) EUMETSAT satellites sensor data. LSA SAF products are mainly oriented to numerical weather prediction, land surface monitoring and climate change communities.

Our main concern in LSA SAF is to develop an operational algorithm for retrieving vegetation parameters on a global scale using SEVIRI/MSG and AVHRR3/EPS data. LSA SAF Vegetation Products (for external users) are the fractional vegetation cover (FVC) and leaf area index (LAI). These products will be delivered over the full MSG disk (mainly covering Europe and Africa) at 3-km spatial resolution. FVC refers to the surface cover by vegetation whereas LAI refers to the volume of vegetation in the three-dimensional space. Both of them provide us with complementary information of the vegetation canopy for description of both land-surface processes and land-atmosphere interactions. FVC and LAI are primary parameters in land-surface parameterisation schemes employed in Soil-Vegetation-Atmosphere Transfer models, which are used in Global Circulation Models of atmosphere for forecasting weather and climate. They are also parameters of primary interest for a range of Land Biosphere Applications such us environmental management, land use and land cover change, hydrology, natural hazards, desertification and drought conditions monitoring.

The synergistic use of SEVIRI (sun varying data) and AVHRR3 (view varying data close the principal plane) will offer an innovative directional sampling of the Bidirectional Reflectance Distribution Function (BRDF) thanks to concomitant multiple viewing and illumination geometries (Van Leeuwen and Roujean 2002). Therefore, a very good determination of the anisotropy properties of Earth's surfaces is expected, thus improving the accuracy of the estimates derived from next generation EUMETSAT systems.

Since the retrieval of biophysical parameters from coarse resolution satellites is one of the major issues in remote sensing several methods have been developed to estimate them taking into account as much as possible also directional effects. The currently used approaches can be divide in two large groups (Weiss and Baret 1999), semi-Empirical Relationships based on Vegetation Indices (ERVI) and methods based on Physical Model Inversion (PMI). Semi-empirical relationships have been established between vegetation indices and biophysical parameters (Asrar et al. 1985). Vegetation indices are designed to maximize sensitivity to the vegetation whilst minimizing confusing factors such us soil background or atmospheric effects. However, vegetation indices are strongly affected by the sun/view geometry, limiting thus the usefulness of semiempirical approaches. In order to minimize these perturbing factors and maximize the confidence of the relationships with the biophysical parameter, optimal geometries have been determined (Roujean and Bréon 1995). The performance of this method can be improved by combining spectral and directional information, for instance obtaining vegetation indices in an optimal configuration (e.g. sun at zenith and view at nadir for FVC retrieval) by using kernel-driven BRDF models, as it was shown on airborne data (Roujean et al. 1997) and satellite data (Roujean and Lacaze 2002). The main limitations of this approach comes from the limited amount of information used, mostly red and infrared spectral information, when compared to the number of input variables that determine the radiative regimen within the canopy (Baret and

Guyot 1991). On the other hand, model inversion consists of determining the set of parameters (biophysical variables of interest) that minimize the distances between the modelled and measured reflectance. This approach mostly applies to both spectral and directional domains (Pinty et al. 1990, Knyazikhin et al. 1998, Bicheron and Leroy 1999). Methods based on the inversion of a BRDF model are theoretically powerful and it can be potentially applied to varying surface types. Furthermore, the use of multi-angular data decreases the dispersion and saturation of the LAI increasing the quality and accuracy of retrieved parameters, especially in geometrically complex canopies (Zhang et al. 2000). The primary limitation is the difficulty in determining appropriately all the input parameters of the model, along with the fact that a different set of parameters may yield to very similar spectro-directional signatures leading to unstable solutions (Weis and Baret 1999). Furthermore they are more complex and time-demanding than the previous one. In order to take advantages of both approaches and to use a single algorithm irrespectively of the BRDF sampling (in a first stage only MSG data will be available) we have considered in parallel these two main approaches to retrieve FVC and LAI (see section 2 for details). In this study we are focused only in the physical model inversion approach, which is named directional spectral mixture analysis (DISMA).

• Objectives

Our main task during the development phase of the LSA SAF project is to develop a prototype to evaluate the operationally, and feasibility of the algorithm to retrieve FVC and LAI, along with determining possible error sources. The DISMA prototyping, which is described hereafter, was previously applied to airborne POLDER data over a well-known crop area, showing very good agreement with ground truth (Garcia-Haro et al. 2003). However, the results obtained at 20m spatial resolution over homogenous plots can be hardly extrapolated to spatial resolution of kilometres over the global range of biomes. Furthermore, some questions remained still unclear such us the determination of some important fixed parameters of the model.

During this visiting scientist stage, our main objective was to evaluate the performance of the DISMA prototyping algorithm applied to POLDER/ADEOS satellite data. To fulfil this objective our work was twofold:

- Adaptation of the DISMA prototyping for its use on a global scale: Definition of the inputs parameters of the DISMA model, in particular, soil BRDF, leaf reflectance and clumping index.
- Comparison of DISMA estimates against standard LAI POLDER products derived using different methodologies. The inter-comparison encompasses a wide range of biomes, especially those existing in Europe and Africa, with full variation of FVC and LAI values.

2.DISMA PROTOTYPING ALGORITHM

2.1 OVERALL PROTOTYPING ALGORITHM

In order to accomplish the retrieval of vegetation parameters with the EUMETSAT new generation systems a prototyping algorithm (figure 1) has been designed, which incorporates the two mains approaches aforementioned (Camacho-de Coca et al. 2002).

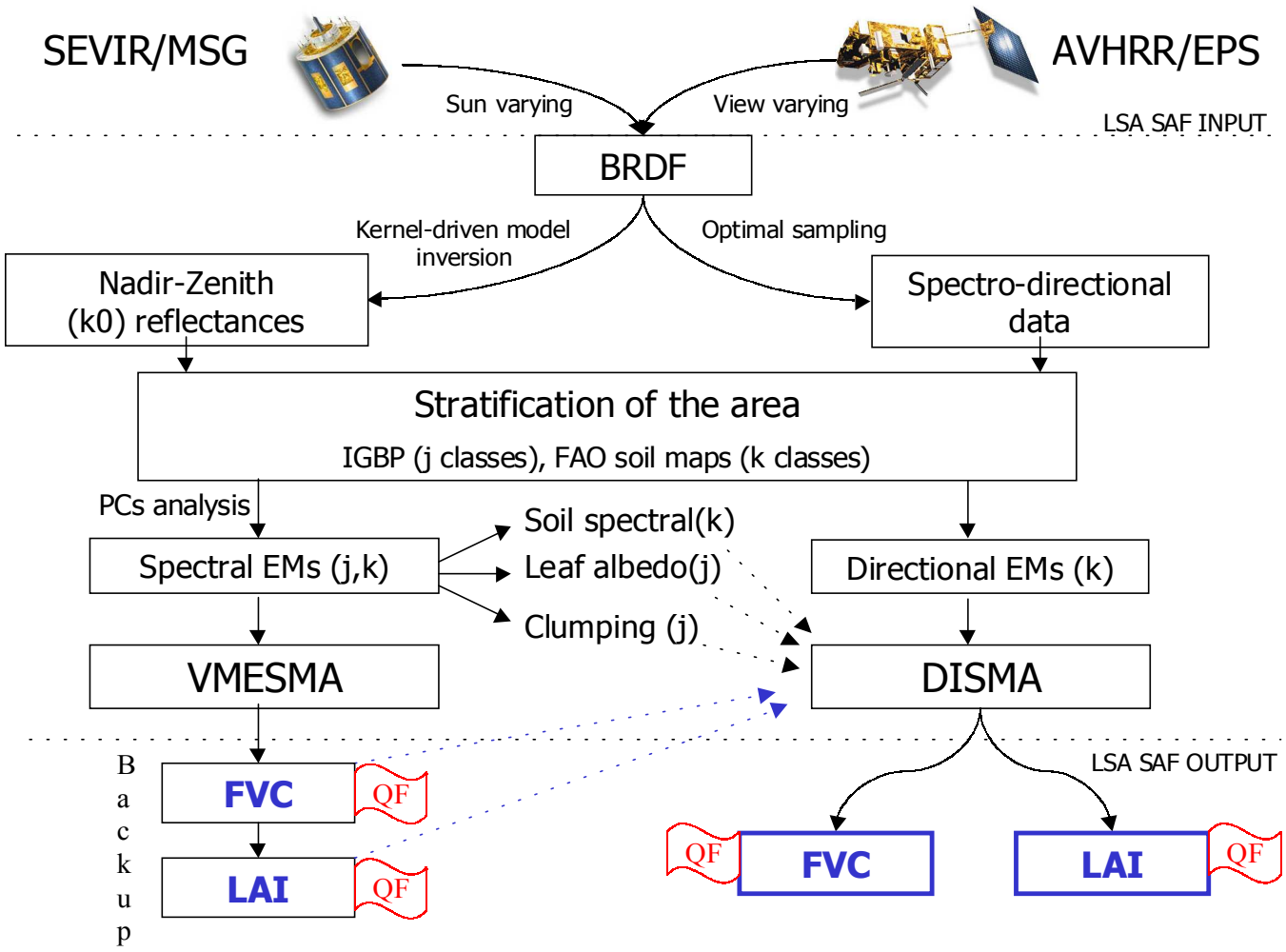

Figura 1. Flow diagram of the MSA and EPS prototype algorithm for retrieving FVC and LAI (QF stands for Quality Flag, and EM for End-Member)

The proposed algorithm is based on the complementary use of an optimised spectral mixture analysis (VMESMA) (Garcia-Haro et al. 2003b, Camacho-de Coca et al. 2003) and the inversion of a physical-based canopy reflectance model (DISMA) (Garcia-Haro et al. 2002). The main steps of the prototype are the following:

• First Step – The **segmentation** of the study area (IGBP land cover map, FAO soil map), which allows the partitioning of the scene into different categories as a function of its spectral and directional attributes. The stratification of the scene subareas is a critical step to improve the accuracy of the derived biophysical products. The segmentation will also allows for selective analysis (e.g. to concentrate the analysis on problematic areas while keeping previous outcomes in well-modelled areas) and eases the iterative improvement of model inputs.

• Second Step – The previous segmentation of the area allows us to select the best subsets of model inputs, termed **Spectral and Directional endmembers (EMs)**, according with landscapes units in order to improve the model performance. Principal component analysis (PCs) will allow determining the set of spectral EMs for each soil and vegetation class, which

are inputs in the VMESMA algorithm. This prior analysis will also serve to define properly some inputs of the DISMA algorithm such us the spectral soil reflectance or the leaf albedo. The directional EMs for the DISMA algorithm consists in select the best model for the soil directional component.

• Third Step – Two complementary **inversion approaches** are considered for the retrieval of FVC and LAI:

The first approach is a variable and multiple endmember spectral mixture analysis (**VMESMA**) (García-Haro et al. 2003b) by using as input the nadir-zenith (k_0) TOC reflectances provided by layer IA (Météo-France) on a daily and 10-days basis. VMESMA enhances the use of thematic maps (steps 1) providing estimates of the FVC very robust against external factors (illumination, soil background) and canopy shade (Kemper et al. 2000). The retrieved FVC will be then used to derive the LAI corrected of clumping as in Roujean and Lacaze (2002). This robust and operational methodology has been satisfactorily tested on both airborne POLDER data, acquired during the DAISEX campaign of the European Space Agency, and synthetic SEVIRI data provided by Météo-France (Camacho-de Coca et al. 2002). This approach to derive LAI is closely related with the vegetation indices ones; It use only spectral information on an ideal geometry to derive FVC using 3 spectral channels, and then applies a semi-empirical relationship to derive LAI. The main improvement comes from the expected higher accuracy in the FVC retrieved with a variable mixture analysis.

Using the normalised reflectance the main drawback of the SMA approach, which is related to the different acquisition geometry in the data, is solved. However, linear mixture does not take into account neither multiple scattered radiance nor crown transparency and, thus, information related with structural parameters such us the LAI or the leaf orientation is ignored. Therefore, a bias in the estimates should be expected in the VMESMA approach. Furthermore, as the VMESMA algorithm relies on normalised data, it does not fully exploit the information provided by the rich directional sampling available when merging SEVIRI and AVHRR capabilities

The second approach -directional spectral mixture analysis (**DISMA**)- based on a physical model inversion aims to take benefit of the directional information and solve the limitations of the SMA approach. For that, we propose a hybrid model, which combines the geometric optics of large-scale canopy structure with principles of radiative transfer for volume scattering within individual crowns. The model formalism and the volume scattering formulation are similar to the GHOST model (Lacaze and Roujean, 2001), but the between-crown gap probability is formulated in terms of FVC and a geometrical variable associated with the shape of plants (see details in section 2.2). In addition, the model allows us to derive other parameters such us the entire BRDF distribution, albedo or absorptance, including the relative contribution of vegetation and soil (see Garcia-Haro et al. 2002).

• Fourth Step – After the inversion procedure, an error assessment will be conducted and the quality flag of the products defined. It is expected that the inversion of the DISMA model will be dependent of the available directional sampling. For that reason, we used the FVC and LAI derived from the VMESMA algorithm as a backup for the DISMA algorithm, due to VMESMA uses only the spectral normalised reflectance, thus it works independently of the

directional sampling available, whereas DISMA may work better as the directional sampling increase.

2.2 DISMA FORMULATION

The reflectance of an individual pixel is assumed to consist of an area weighted linear combination of the soil and vegetation contributions:

$$R = R_v + R_s \tag{1}$$

The vegetation reflectance is expressed as a sum of single scattering (ss) and multiple scattering (ms) reflectances (Hapke 1981, Lacaze and Roujean, 2001):

$$R_v = \frac{\omega}{4}\frac{1}{\mu_s \mu_v}\cdot\left\{P(\xi)\, I_{ss} + \left[H(\mu_s)\, H(\mu_V) - 1\right] I_{ms}\right\} \tag{2}$$

where ω is the leaf scattering albedo, $\mu_{s,v} = \cos\theta_{s,v}$, ξ is the phase angle, and the factors I_{ss} and I_{ms} model the proportion of radiation flux which is single/multiple scattered by foliage elements on the downgoing and outgoing optical pathways as a whole. The Chandrasekhar function $H(\mu_{s,v})$ is used to compute multiple scattering (Hapke, 1981). $P(\xi)$ is a turbid medium phase function (Ross 1981, Lacaze and Roujean 2001).

The proposed model assumes that the geometrical component and the volume component of the radiation fluxes can be decoupled in such a way that the flux interception of radiation can be expressed as follows:

$$I_{ss} = I_{ss,vol}\cdot I_{ss,geo} \qquad I_{ms} = I_{ms,vol}\cdot I_{ms,geo} \tag{3}$$

The monodirectional foliage projection G-function (Ross, 1981) controls the volume component depending on the within-crown element distribution, whereas the external geometric component depending on the crown shape and dimension is evaluated using an average theory of the gap probability.

• Volume component

The volume single/multiple scattered component can be described using the Beers' law:

$$I_{ss,vol} = \frac{1}{\Delta}\left[1 - \exp(-\Delta\ \mathrm{LAI}\ \Omega_E\ \gamma / g_c)\right] \tag{4}$$

$$I_{ms,vol} = \frac{1}{\Delta'}\left[1 - \exp(-\Delta'\ \mathrm{LAI}\ \Omega_E\ \gamma / g_c)\right] \tag{5}$$

where Ω_E is the clumping index of the shoots, which quantifies the level of foliage aggregation within the tree crown. LAI is the scene leaf area index defined as half the total leaf area per unit ground surface area, g_c denotes the fractional vegetation cover and γ is a band-specific factor, which was assumed to be dependent on the leaf transmittance (e.g. Bégué, 1992). Assuming plants with similar foliar density in the scene, LAI/g_c represents an average value of the LAI of individual plants. This term is more pertinent to describe crown

trees transparency than scene LAI. Δ denotes the (bidirectional) normalised extinction coefficient for singly scattered radiance.. For the once scattered radiation, there exits a coupling between the downgoing and outgoing optical pathways, so-called the hot spot effect (Hapke et al. 1996, Qin and Goel 1995). We are adopted the expression suggested by Roujean (2000) that takes into account the hot spot:

$$\Delta = \sqrt{\frac{G_s^2}{\mu_s^2} + \frac{G_v^2}{\mu_v^2} - 2\frac{G_s}{\mu_s}\frac{G_v}{\mu_v}\cos\xi} \tag{6}$$

where $G_{s,v}$ is the well-known function defined by Ross (1981) to represent the mean monodirectional foliage projection, which depends on the LAD. Hence, the shape of the hot spot will be controlled by the foliage orientation. For multiple scattered radiation, where the hop spot effect is not present, the equation reduces to the classical expression Δ':

$$\Delta' = \frac{G_s}{\mu_s} + \frac{G_v}{\mu_v} \tag{7}$$

• Geometric component

The geometric component of the single scattering $I_{ss,geo}$ is determined by the between-crown light penetration and the visibility of illuminated objects. This component is particularly relevant for discontinuous canopies. For example, forest reflectance is dominated by the contrast between the sunlit and shaded components, especially in the visible parts of the spectrum. One question that arises is to describe the contribution of shaded and illuminated ground and crown, even when overlapping complicates the generalisation for denser canopies. Intercepted fluxes were formulated in terms of horizontal projection of the crown. Let denote by $P_0(\theta)$ the (between-crown) monodirectional gap fraction, which corresponds to the fraction of soil seen in the direction θ (Nilson, 1971). It is a biophysical variable of prime interest for remote sensing since it directly determines the single scattering process in the radiative transfer (Weiss and Baret 1999). LAI is strongly related to the monodirectional gap fraction. In fact, P_0 at particular directions provides an indirect way to estimate LAI and fAPAR (Weiss and Baret 1999). For homogeneous Poisson distribution, the probability of observing the ground under the tree crowns in any given pixel approaches to (Jasinski and Eagleson, 1989):

$$P_0(\theta_s) = (1 - g_c)^{(\eta+1)} \tag{8}$$

where η is defined as the ratio of ground projected shadow to plant area. It absorbs all the geometric factors, which relate canopy area to shadowing area into only one variable. Its analytical expression for the most common geometrical bodies is provided in Jasinski and Eagleson (1990). For example, for the case of square cylinders, we have $\eta = \tan\theta / b$, where *b* is the similarity parameter, defined as the ratio of the mean width D to the mean height H. The probability of having sunlit ground P_{ig} and viewed ground P_{vg} can be expressed as follows:

$$P_{vg} = P_0(\theta_v) \qquad P_{ig} = P_0(\theta_s) \tag{9}$$

A functional relationship can be also found between subpixel shaded ground P_{sg} and fractional vegetation cover:

$$P_{sg} = 1 - g_c - (1 - g_c)^{(\eta_s + 1)} \tag{10}$$

Logically, the vertical crown cover projections in the view and sun directions are given by:

$$P_{vc} = 1 - P_0(\theta_v) \qquad P_{ic} = 1 - P_0(\theta_s) \tag{11}$$

The above equations are applicable at large sampling scales, when imaging stands resolutions greater than the size of the tree crowns. In order to confirm these mathematical relationships, different nadir images were simulated by means of a canopy reflectance model (García-Haro and Sommer 2002). The spatial distributions of subcanopies, dimensions, density and sun geometry were systematically altered, allowing us to evaluate the conditions in which the proposed parameterisation is applicable. The study revealed a close agreement between the values of P_{sg} derived using the simulation and the values obtained using Eq. (10).

The probability of observing sunlit crown when P_{ic} and P_{vc} are not correlated is simply the product of both probabilities $P_{ic}P_{vc}$, where P_{ic} controls the amount of light intercepted by crowns and P_{vc} controls the contribution of visible crowns to the scene radiance. However, hot spot kernels are necessary to account for the correlation between the two gap probabilities along sun and view directions. They should be unity when the sun and view positions align (i.e. at the hot spot) and vanish when the phase angle is large enough. For large pixels and heterogeneous canopies the hot spot effect seems to be dominated by the radiation transmission between the gaps of macro-scale elements forming the landscape such as groups of trees instead of micro-scale elements like needles (Lacaze et al. 2002). Direct calculations for the joint probability are, however, very complicated and require the use of certain simplifications. For example, they usually assume known the distribution of gap size inside and between tree crowns (Chen and Leblanc 1997) or use a simple prescribed representation of crown trees sizes, shapes and distributions (Li and Strahler 1992, Qin et al. 1996). A hot spot kernel, $F_c(\xi)$, obtained from the overlap function between viewing and illuminated shadows as projected on the background (Li and Strahler 1992) has been then used to take into account the hot spot effect for once-scattered radiation. The geometric components of the single and multiple scattering are expressed as:

$$I_{ss,geo} = P_{ic}P_{vc} + [P_{ic} - P_{ic}P_{vc}]F_c(\xi) \tag{12}$$

$$I_{ms,geo} = P_{ic}P_{vc} \tag{13}$$

• Soil component

The soil contribution, R_s, is expressed as the product of soil bidirectional reflectance, γ_s, and vegetation transmittance T:

$$R_s = T\,\gamma_s \tag{14}$$

The vegetation transmittance can be expressed as the sum of the probability that a solar ray beam will reach the ground without intercepting any crown T_{geo} plus the probability of intercepting a crown without hitting any foliage element, i.e.:

$$T = T_{geo} + (1 - T_{geo})\, T_{vol} \tag{15}$$

The following expressions were considered for the transmissions:

$$T_{vol} = \exp(-\Delta\ \mathrm{LAI}\ \Omega_E\ \gamma / g_c) \tag{16}$$

$$T_{geo} = P_{ig} P_{vg} + \left[P_{ig} - P_{ig} P_{vg}\right] F_G(\xi) \tag{17}$$

where F_G is a hot spot kernel, which tends to zero when the sun and view directions are fare apart. In this study, it has been parameterised using a simple analytical expression. The hot spot kernels F_c and F_G are similar to the hot spot function proposed by White et al. (2001), which match the hot spot region measured in many BOREAS sites (Leblanc et al. 1997).

Model neglects side scattered diffuse radiation incident on ground surface after multiple scattering with leaves of neighboring plants. Field measurements and radiosity models all show that the side scattered light can be very significant (Roberts et al. 1990, Borel and Gerstl 1994). The model is thus generally accurate for visible part of the solar spectrum, but less accurate at near-infrared wavelengths at which multiple scattering in plant canopies is the strongest within the solar spectrum. These non-linear effects exert a strong impact at shrub scale but they can be considered small at landscape scales when there is an horizontal mixing of vegetation types or materials (Asner et al. 1998; Qin and Gerstl 2000).

• Diffuse component

The above equations consider only the contribution of direct radiation to the reflectance. Considering also the presence of skylight irradiance, the reflectance can be expressed as a sum of the direct and isotropic diffuse components:

$$R = (1 - k_d)\, R_{direct} + k_d\ R_{diffuse} \tag{19}$$

where the component of diffuse reflectance was calculated as the average of the measurements in the principal plane. k_d denotes the fraction of diffuse irradiance, which was parameterised as follows (Lacaze and Roujean 2001):

$$k_d = \frac{0.09}{0.09 + \mu_s} \tag{20}$$

3. METHODOLOGY

3.1 POLDER/ADEOS DATA

• Polder database

The POLDER instrument is described in Deschamps et al. (1994). It is composed of three major components: a CCD matrix detector, a rotating wheel carrying the polarizers and filters, including one for measuring dark current, and a wide field-of-view (FOV) telecentric

lens; The CCD detector is composed of 288×384 pixels, the 8 spectral filters are 443, 490, 565, 670, 763, 765, 865 and 910 nm wavelength centred with a bandwidth of approximately 20 nm, (iii) the FOV was along track and cross track of ±43º and ±51º respectively, with a diagonal FOV of ±57º. The Earth curvature results in surface observation at larger view zenith angles : ± 50° (along track), ± 61° (across track) and ± 70º (in the diagonal). The polarizers are three channels (443, 670 and 865 nm).

The basic inputs for the construction of the BRDF data set is level 2 bi-directional surface reflectances at 443, 565, 670 and 865 nm over the 8 months of POLDER acquisition. The pixels are classified according the 17 biomes of the IGBP classification {1) Evergreen needleleaf forest, 2) Evergreen broadleaf forest, 3) Deciduous needleleaf forest, 4) Deciduous broadleaf forest, 5) Mixed forest, 6) Closed shrublands, 7) Open shrubland, 8) Woody savannas, 9) Savannas, 10) Grasslands, 11) Permanent wetlands, 12) Croplands, 13) Urban and built-up, 14) Cropland/natural vegetation mosaic, 15) Snow and Ice, 16) Barren or sparsely vegetated, 17) Water bodies}, the period of measurement, the NDVI from level 3 synthesis product and the location of the pixel in 5 bands of latitude (90°N-50°N; 50°N-30°N; 30°N-30°S; 30°S-50°S; 50°S-90°S)

The criteria of selection for the pixels are: (1) The number of view on the track shall be higher or equal to 10. (2) The distribution of tracks in the viewing hemisphere. This one is sampled by 8° and the tracks, characterized by the viewing zenith angle of their center, are distributed in the corresponding directional classes. A pixel shall have at least one track in 5 different angular classes during the considered month to be selected. (3) The number of clear tracks collected during the considered month shall be higher or equal to 8. A filtering algorithm developed in the frame of Level 3 "Land Surface" processing line for POLDER2 is applied. It allows removing the residual cloudy tracks and data perturbed by a high content of aerosols using a temporal analysis of directional observations acquired close to the perpendicular plane. We keep only pixels for which the previous criteria 2 and 3 shall remain valid after filtering. At final, 22594 pixels frame the database (Lacaze, 2003).

The DIScover IGBP represents the first opportunity of a global land cover at this resolution. However, the IGBP classification outside the USA is quite inaccurate. The POLDER BRDF proves that, in some pixels, the IGBP vegetation does not fit the surface cover (Lacaze, 2003). Updated land cover classification such us the Global Land Cover GLC-2000[1] will be used instead when available.

Figure 2 shows an example of the BRDF at 670 and 865 nm for two different land cover types. The plots show the high anisotropic behaviour of vegetation canopies. The BRDF is almost symmetrical regarding the principal plane, and very asymmetric regarding the orthogonal plane, showing the highest values in the hot spot domain. The directional signature in the principal plane between ±45º is used as input data for the inversion of the DISMA model (figure 3). However, the DISMA model could be inverted against directional data acquired in other configurations (Garcia-Haro et al. 2003).

[1] http://www.gvm.sai.jrc.it/glc2000/defaultGLC2000.htm

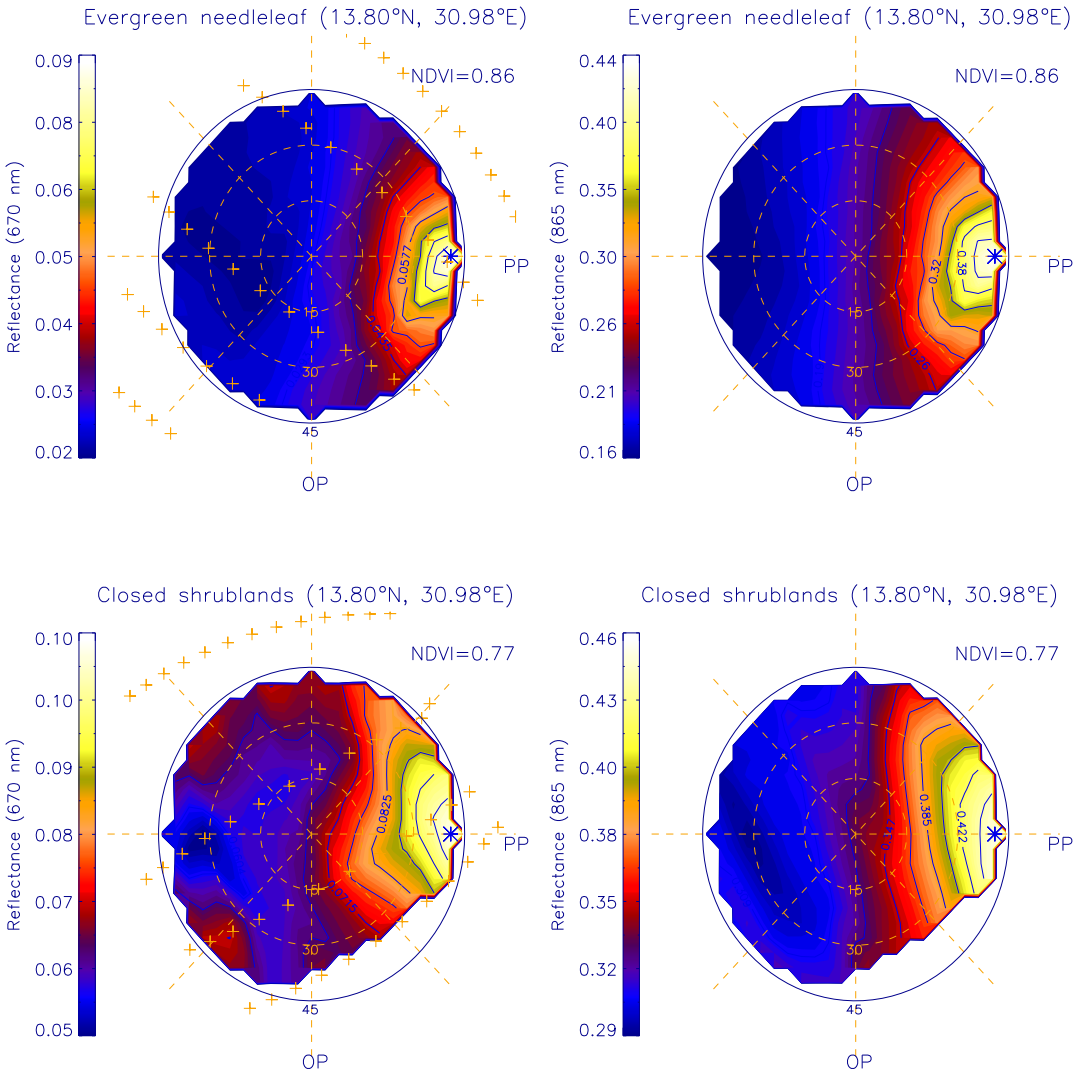

Figura 2. Examples of POLDER BRDF at 670 nm (left) and 800 nm (right) for Evergreen nedleleaf forest (top) and Closed shrublands (bottom). The star represents the sun position and the crossess (on the left side) the viewing geometry.

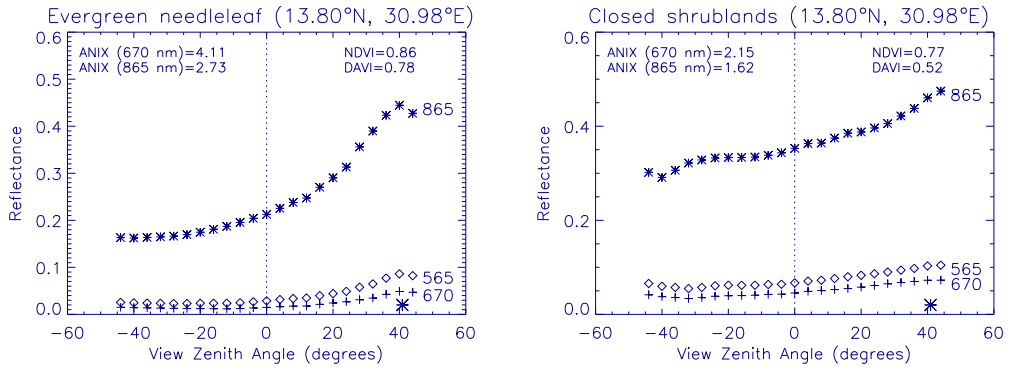

Figura 3. Examples of POLDER BRDF at 670 nm (left) and 800 nm (right) for Evergreen nedleleaf forest (top) and Closed shrublands (bottom). The star represents the sun position.

• LAI POLDER global products

In order to evaluate our algorithm two different LAI POLDER products have been used:

(1) The first one corresponds to the category of empirical relationships with vegetation indices (ERVI). The method is described in Roujean and Lacaze (2002). First, the BRDF data is used to derive the 3 parameters of the kernel-driven Roujean et al. (1992) model. After that, the nadir-zenith (k_0) reflectance is used to compute the vertical difference vegetation index (DVI_0). The FVC is then obtained from a simple empirical relationship FVC-DVI_0. Then the LAI is related with the FVC by the following relationship:

$$FVC = 1 - \exp\left\{-b\left[G(\theta_s)/\cos\theta_s\right]_{\theta=0}\Omega LAI\right\} \quad (21)$$

where Ω is the clumping index, and *b* is a parameter related with the leaf albedo. Some hypothesis are required such us randomly oriented leaves (G=0.5) or the value of the *b* parameter (0.945). The clumping index is computed using a relationship with the DVI constrained by two threshold values on the vertical simple ratio, which are fixed empirically (Roujen and Lacaze, 2002). For this approach, we have 10-days LAI global products. We have used the LAI product of April'97 centred in the day 15.

(2) The second one corresponds to the category of physical model inversion. The method is described in Bicheron and Leroy (1999). The canopy is modeled as a homogeneous turbid medium, limited by a soil layer also homogeneous. This assumption could be unrealistic in some situations (for instance in classes with prominent vertical structures). Nevertheless, the approach provides a sound physical representation of the average properties of soil-vegetation layer. In addition, it should provide a sensitive improvement relative to the use of semi-empirically relationships due to the wide range of biomes and geometries where it could be applied. The BRDF model is a slightly modified version of the Kuusk (1995), which is derived from the Nilson and Kuusk (1989) model for the description of single scattering (including hot spot), the SAIL (Verhoef, 1984) model for multiple scattering, the PROSPECT (Jacquemoud and Baret, 1990) model for optical properties of leaves, and Price (1990) and Walthall et al. (1985) for modelling the soil BRDF. A neuronal network approach is used to invert the model. The main outputs of the inversion are the LAI and the chlorophyll content; the soil spectral parameter (a1) and the structural parameter (leaf size to canopy height) are free parameters and thus also model outputs. The LAI product derived using this method is monthly. In this work, we have used the April'97 product.

In order to perform the evaluation of the DISMA prototype a comparison of LAI/FVC DISMA estimates against POLDER products has been undertaken. For that, we have selected 40 samples with NDVI ranging from 0.05 to 0.85 for each one of the 6 different IGBP classes selected, which are: Evergreen Needleleaf Forest, Evergreen Broadleaf Forest, Mixed Forest, Closed Shrublands and Barren of Sparsely Vegetated. The location of the samples used in this study is shown in figure 4.

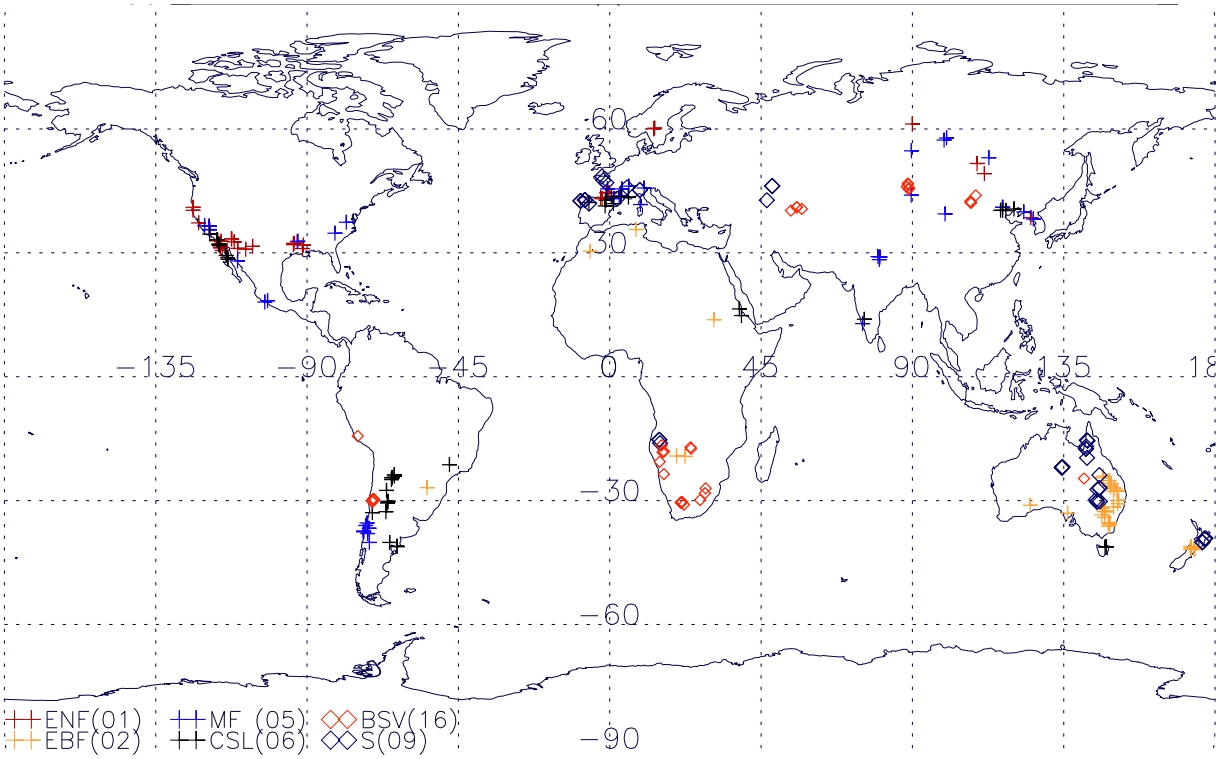

Figura 4. Location of the samples used in this study. Diferent colors and symbols are used for each considered IGPB class: ENF (Evergreen Needleleaf Forest), EBF (Evergreen Broadleaf Forest), MF (Mixed Forest), CSL (Closed Shrublands), S (Savannas) and BSV (Barren and Sparsely Vegetated). The number of the IGBP class is shown in the legend.

3.2 FIXED PARAMETERS DEFINITION

• Selection of the soil BRDF's model

For the soil model spectral-directional reflectances, we have chosen the coupled Price-Walthall model. The suitability of this model for retrieving biophysical parameters by inversion of a canopy reflectance model was demonstrated in Bicheron and Leroy (1999) using airborne POLDER data. The soil spectra is modelled by considering it as a sum of a small number of basis functions (Prince, 1990) whereas the directional behaviour is modelled by using the parametric Walthall's BRDF model (Walthall et al. 1985).

The Price-Walthall BRDF models reads:

$$\rho(\lambda,\theta_s,\theta_v,\phi) = f(\lambda)\cdot g(\theta_s,\theta_v,\phi) \tag{22}$$

where

$$f(\lambda) = a_1 f_1(\lambda) + a_2 f_2(\lambda) + a_3 f_3(\lambda) + a_4 f_4(\lambda) \tag{23}$$

$$g(\theta_s,\theta_v,\phi) = 1 + W_a\theta_s\theta_v\cos\phi + W_b{\theta_s}^2{\theta_v}^2 + W_c({\theta_s}^2 + {\theta_v}^2) \tag{24}$$

The Price-Walthall model has 4 spectral parameters and 3 directional parameters. This model could be optimised for remote sensing application reducing the number of free parameters. Two optimised Price-Walthall models were proposed by Quesney et al. (2001) for its use in the chain of POLDER2 biophysical products. This optimisation of the Price-Walthall model is based on the analysis of more than 5000 POLDER/ADEOS BRDFs of semi-arid areas (0.15<NDVI(t)<0.3). The parameterisation is written as follows:

$$\rho(\lambda,\theta_s,\theta_v,\phi) = a_1 f_1(\lambda)\cdot(1+W_a(\theta_s)\cdot\theta_s\theta_v\cos\phi+W_b(\theta_s)\cdot\theta_s{}^2\theta_v{}^2) \quad (25)$$

where

- $W_a = 1.09 - 2.27\theta_s + 2.09\theta_s^2 - 0.62\theta_s^3$
- $W_b = -2.79 + 8.40\theta_s - 7.75\theta_s^2 + 2.29\theta_s^3$

and the Price function takes the following values:

- f_1(565 nm)=0.4561
- f_1(670 nm)=0.6168
- f_1(865 nm)=0.7709

Using this parameterisation, the spectral soil component is controlled by one parameter (a1) and the directional component is driven by the sun and view angles. This approach provides an error lesser than 4% for the 90% of the analysed POLDER pixels (Quesney et al. 2001). However a slight modification has been introduced on the spectral part of the model. The Price-Walthall (a1) parameter has been considered wavelength dependent (a1(λ)), and obtained by fitting spectrally the model to the POLDER BRDF of samples with a NDVI<0.2. This improves slightly the adjustment between model and observations. In the MSG algorithm the spectral soil component will be fitted to the soil EMs extracted using a soil map during the execution of the VMESMA algorithm. The angular part of the model (directional EM) could be improved considering other models such us the RPV model (Rahman et al. 1993). Nevertheless, the simply Walthall model provides an acceptable representation of the directional soil reflectance, at least for coarse spatial resolution data (see figure 5).

Note in figure 5 that the simple Whalthall's model does not fit well the soil directional signature when the anisotropy is high. This could translate into a bias in the DISMA outcomes due to the difference between modelled and measured reflectances could be compensated by an increasing vegetation amount giving unrealistic results. Nevertheless, most of the samples studied with NDVI<0.2 are well fitted using the Walthall model.

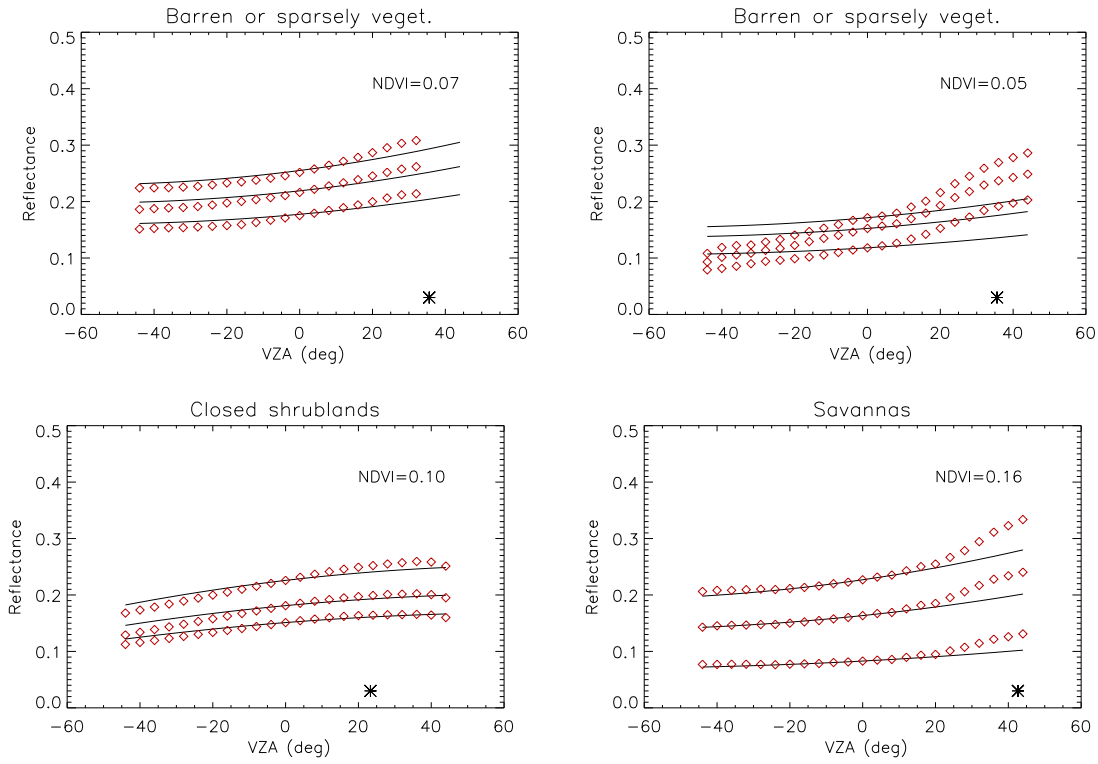

Figura 5. Soil POLDER directional signatures (diamonds) and the modelled Price-Walthall signature (lines) for different samples (NDVI<0.2) corresponding to the IGBP Barren or sparsely vegetation (top), Closed shrublands (bottom left) and Savannas (bottom right). The spectral parameter of the Price-Walthall model has been fitted to the nadir view. The star represents the sun zenith angle.

For each IGBP class, we have selected 5 samples with NDVI<0.2 and obtained its corresponding soil spectral parameter (a1(λ)). For the inversion of DISMA, the main value, the highest (brighter soil) and the lowest (darker soil) value are used as input of the DISMA (the main values of a1 used in the inversion are shown in Table 1). The solution corresponds to that with the lowest RMS error. Figure 6 shows the RMS error as a function of the soil spectral parameter (mean, dark or bright) used. In most of the cases the mean value gives the lowest RMS. The RMS ranges typically between 0.01 and 0.02 for all the IGPB classes, which shows the goodness of the fit.

Table 1. Mean soil spectral parameter used for soil modelling

	a1(565)	a1(670)	a1(865)
IGBP 01	0,23	0,25	0,3
IGBP 02	0,3	0,31	0,35
IGBP 05	0,26	0,23	0,24
IGBP 06	0,27	0,24	0,26
IGBP 09	0,22	0,23	0,25
IGBP 16	0,31	0,28	0,28

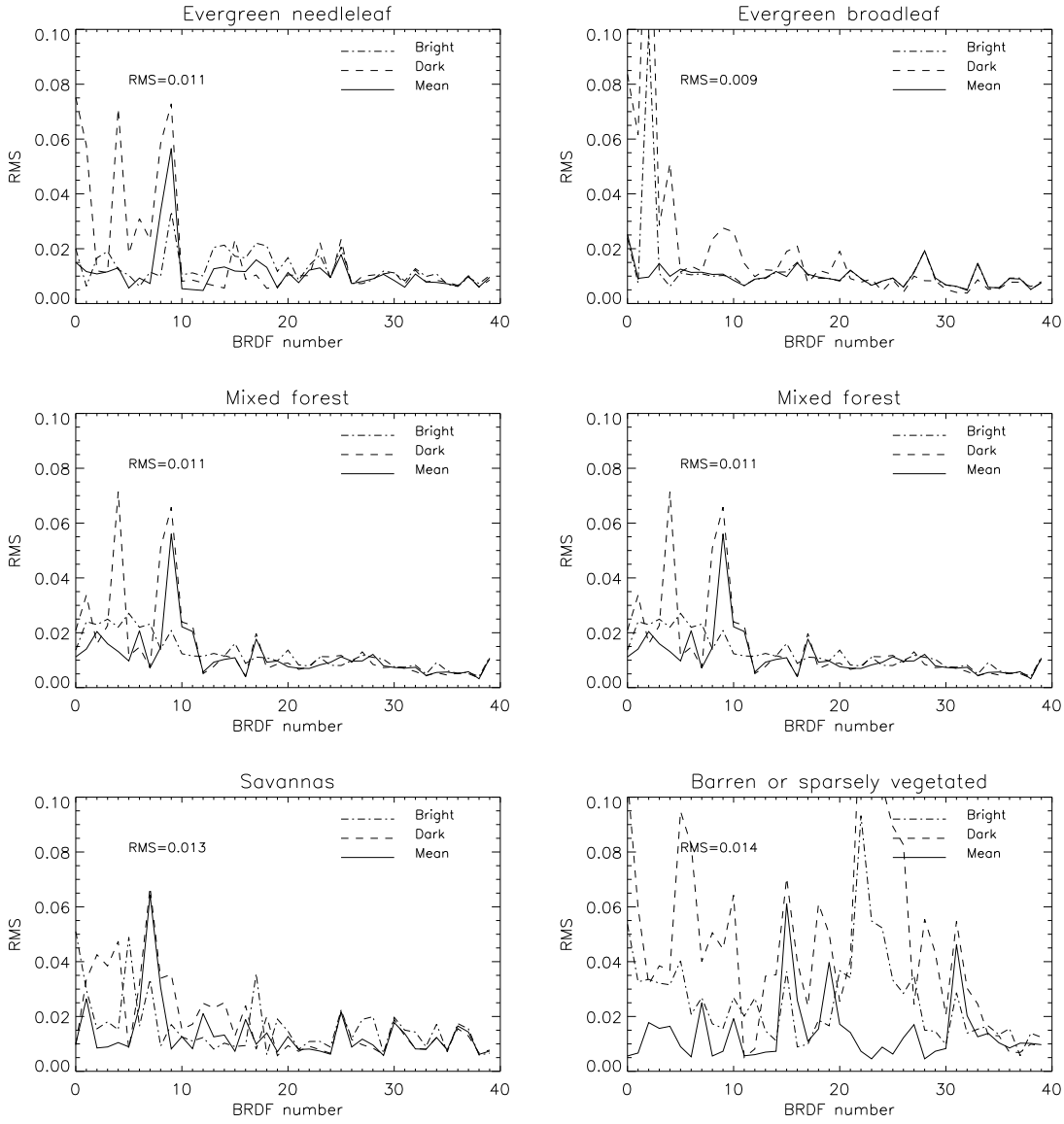

Figura 6. RMS of the fit using three different soil spectral parameter (mean, dark and bright) for the considered IGBP classes. BRDF samples are ordered from low to high NDVI.

• Leaf albedo estimation and clumping index

A method to estimate the leaf albedo automatically from the data has been proposed. The method relies on the assumption that pixels presenting a negligible contribution of soil backgroung can be found in the scene. In these pixels, Eq. (2) can be inverted in order to retrieve ω using an iterative method. Results have indicated the adequate convergence of the method, providing reasonable results irrespectively of the data set considered. The 5 selected BRDF samples corresponding to the highest NDVI class (NDVI>0.8) have been used to retrieve different leaf albedo. The given solution uses the leaf albedo that provides the lowest RMS error. This procedure will be optimised during the process of EMs selection. Typical values for albedo are shown in table 2. Note that 6 different values for leaf albedo obtained varying the LAI in Eq. (2) have been used. A uniform leaf angle distribution has been used.

Table 2. Example of leaf albedo (ω) used in DISMA

	ω(565)	ω (670)	ω (865)
IGBP 01	0,1	0,04	0,71
IGBP 02	0,05	0,03	0,55
IGBP 05	0,05	0,04	0,52
IGBP 06	0,16	0,1	0,66
IGBP 09	0,1	0,06	0,71
IGBP 16	We use the IGBP 06 values		

In addition the clumping index has been estimated by using the method proposed in Roujean and Lacaze (2002). The estimated values ranges between 0.6 and 1.0 for samples with NDVI higher than 0.6.

• Admitted solutions

The last step before the execution of the algorithm was the definition of a domain of physical solutions and the use of a prior information in order to reduce the time of computation. The inversion of the DISMA algorithm is carried out simultaneously by using the spectral and directional information. The inversion procedure consists in determining the set of parameters (LAI, FVC) that minimise the distance between observation and modelled values. To define the domain of admitted solutions in the inversion procedure we have used the same exponential relationship used to retrieve FVC from LAI in the POLDER level 3 algorithm[2]. Thus, the admitted solutions are constrained by this exponential function as it is shown in figure 7.

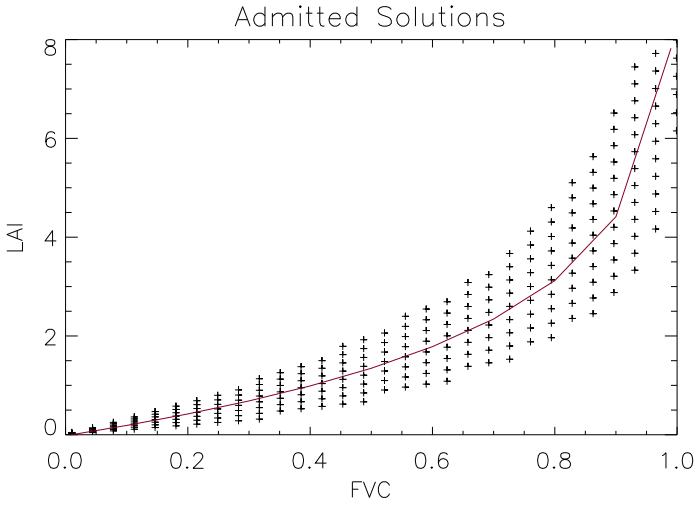

Figure 7.- Admitted solutions in the inversion of DISMA

Before the execution of the DISMA algorithm a priori information is considered to determine the interval where solutions must be located. We applied a simple SMA to obtain a first approach to the FVC value. A distance lower than 0.2 of the first FVC value restricts the final domain of solutions. In the MSG algorithm this strategy will be also employed using the FVC and LAI values derived from VMESMA algorithm to define the bidimensional bounds in the solution domain.

[2] http://smsc.cnes.fr/POLDER/SCIEPROD/lsp2algol3.htm

• Model inversion

The inversions are achieved simultaneously for all spectral bands, i.e. by coupling the spectral and directional data available. The variables to be retrieved are LAI and FVC (g_c). Given BRDF values $\mathbf{R_{meas}}$(i=1,...n), representing the conditions of observation (i.e. wavelengths and view and illumination geometries), the retrievals are performed by comparing observed and modeled $\mathbf{R_{DISMA}}$ (i=1,...n) BRDFs. The comparisons are evaluated for a full set of prescribed canopy realisations (g_c , LAI) that cover a range of expected natural conditions as describe before (see figure 7). Those pairs for which the canopy model generates inputs comparable with measured data, within the limits of accuracy of data, i.e.:

$$(R_{meas} - R_{DISMA})^T W^{-1} (R_{meas} - R_{DISMA}) < N \qquad (23)$$

are considered as acceptable solutions, where **W** is the covariance matrix of the measurements. The diagonal elements of **W** are the variance, which should account for both data uncertainty and unquantified errors associated with the simplifying assumptions of the theoretical model. The information about uncertainty and their correlation may improve the accuracy of retrievals, as shown in Combal et al.(2002).

The distribution of solutions defines a domain for FVC and LAI around the "true" values. Mean values of FVC and LAI averaged over a set of solutions with lowest RMS (3 cases in this study) are given as solution. This procedure not only increases the numerical stability of the inversion but also enables us to derive the uncertainty and correlation of derived parameters.

4. RESULTS

Once the input definition was completed, the DISMA model was inverted against POLDER measurements of different IGBP classes. The results show the capability of the DISMA model to fit simultaneously spectral and directional reflectance data under very different vegetation amount, from bare soil to densest canopies, for the six considered IGBP classes, confirming the adequate selection of the inputs. Measured and modelled POLDER directional signatures for each considered NDVI level (from 0.05 to 0.85) and IGBP class are shown in the Annex. The comparison of the LAI and FVC values is shown in section 4.1 and 4.2 respectively.

4.1 LEAF AREA INDEX

Figure 8 (on the left side) shows the retrieved LAI values using the DISMA model and the two algorithms -based on empirical relationship with vegetation indices (ERVI) and a physical model inversion (PMI)- described above as a function of the NDVI of the sample. The best fit of the LAI data as a function of the NDVI is plotted in the graphs along with the standard deviation of the data to the fit. Figure 8 (on the right side) shows the relative difference, expressed in percentage, of the LAI values obtained using the different approaches for the 40 samples, ordered from low to high NDVI level, of each IGBP class.

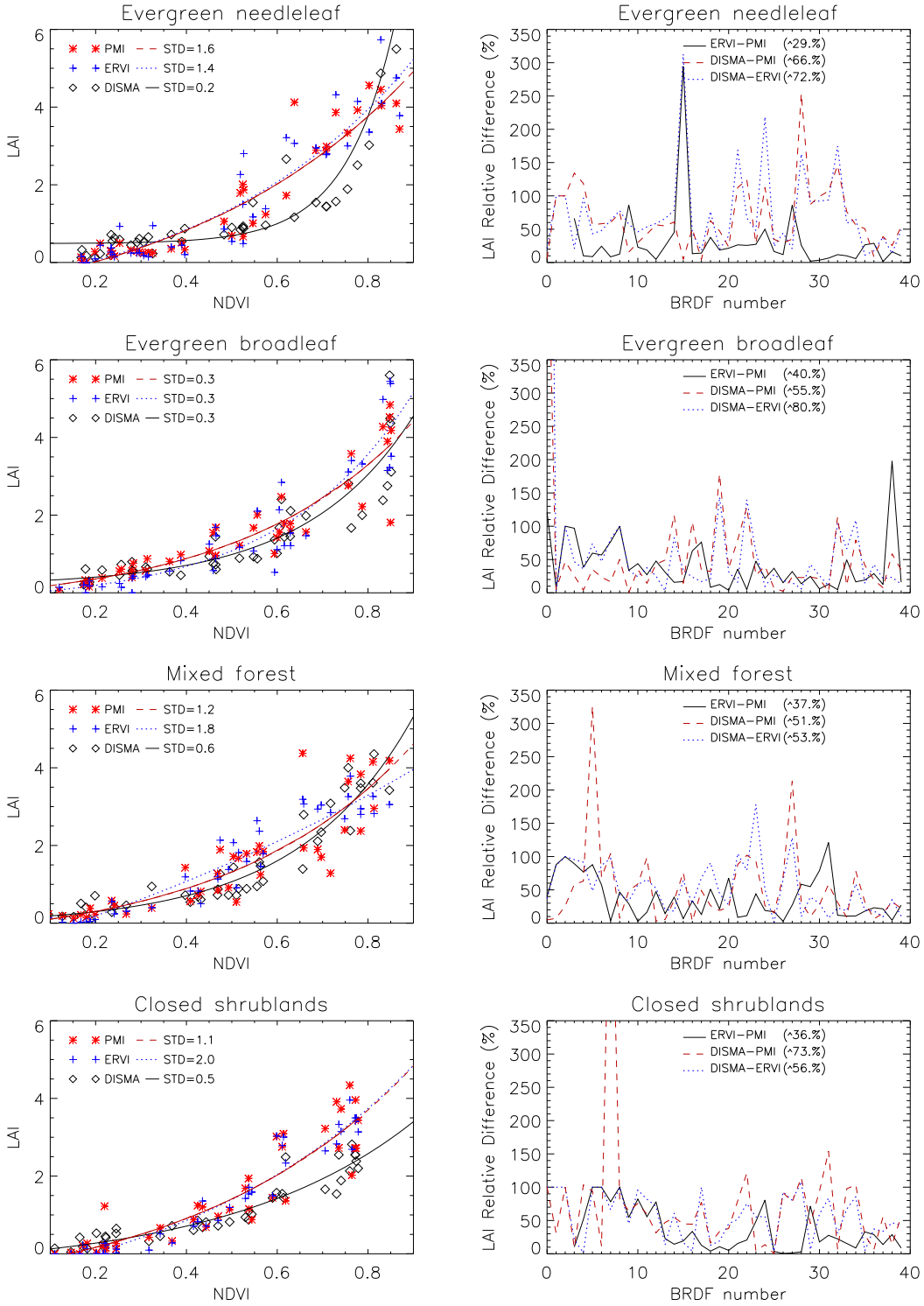

Figure 8.- Retrieved values of LAI using DISMA, PMI, and ERVI approaches (on the left side). FVC relative difference among the different approaches (on the right side)

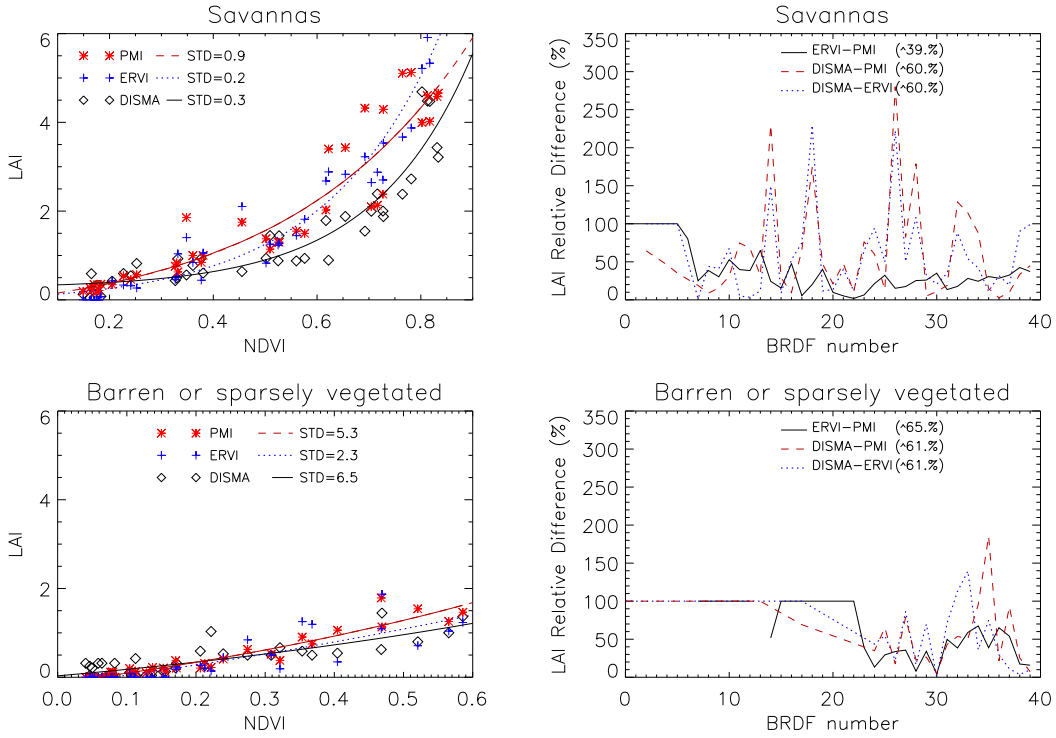

Figure 8.- Continuation.

The comparison of the LAI results show that DISMA model outputs present a similar trend with the NDVI that the ERVI or PMI outcomes, which in general are more correlated between them that with DISMA, specially for the Evergreen needleleaf forest class. In average, the relative difference between the LAI POLDER products is typically of 40%, whilst this difference is typically of 60% when comparing DISMA with ERVI and around 70% when comparing DISMA with PMI LAI values. The standard deviation of the data around the best fit is lower in the DISMA with the exception of the Barren and sparely vegetated class.

In general the DISMA LAI estimates range between the same minimum and maximum values as those derived from PMI or ERVI approach. For the lowest NDVI samples, the DISMA LAI values are very close to zero, although a slight bias regarding the other products occurs in some cases, as can be observed in the Barren or sparsely vegetated class. This error can be partly associated to a deficient characterization of the soil BRDF, in both the spectral part and the directional one due to the Walthall model not always fits well the soil BRDF shape. The spectral parameter of the soil Price-Walthall model will be improved when applied the whole prototyping algorithm to satellite data. Nevertheless, in the final algorithm more accurate BRDF models could be used instead Walthall model. Concerning the highest values of the LAI, the DISMA algorithm provides similar values than the other approaches, which confirms that the dynamic range of DISMA LAI estimates is adequate. Furthermore, the maximum value of retrieved LAI with DISMA is consistent with the expected value according the biome type. For instance, the LAI goes up to 6 for Evergreen needleleaf forest and Evergreen broadleaf forest, it reaches 4.5 for Mixed forest and Savannas, only goes up to 3 for Closed shrublands and it is lower than 2 for Barren or sparsely vegetated. For all the

cases, the maximum value is very close to the ERVI and PMI estimates, with the exception of Closed shrublands where DISMA provides lower values. In principle, DISMA model is physically more suitable to reproduce heterogeneous vegetation canopies than the homogeneous assumption of PMI or ERVI approaches. Major differences occur with intermediate-high vegetation amount, roughly between 0.6 and 0.8 NDVI, where DISMA output underestimates the values of the POLDER products, especially in the Evergreen needleleaf and Savannas classes. Nevertheless, the maximum relative differences are not larger than those exhibit, in some cases, between POLDER and MODIS LAI products (Lacaze, 2002). On the other hand, the standard deviation of the LAI DISMA output around the fit is considerably lower for the DISMA results, especially in the Evergreen needleleaf class. However, at this moment we don't have enough elements to judge if the DISMA LAI results are worse or by the contrary represents better the nature than POLDER product results. For that reason, validation of the DIMSA products on a wider spatial and temporal dimension become of great importance for the final assessment of uncertainties.

4.2 FRACTIONAL VEGETATION COVER

Figure 9 shows the comparison of the FVC values and the relative difference between the different products. The FVC POLDER products have been derived from the LAI products. For the ERVI approach we have inverted Eq. (21) using the same clumping index values used for the DISMA inversion. For the PMI approach we have applied the exponential relationship (FVC=1- exp(-0.5 x LAI)) used in the POLDER level 3 algorithm.

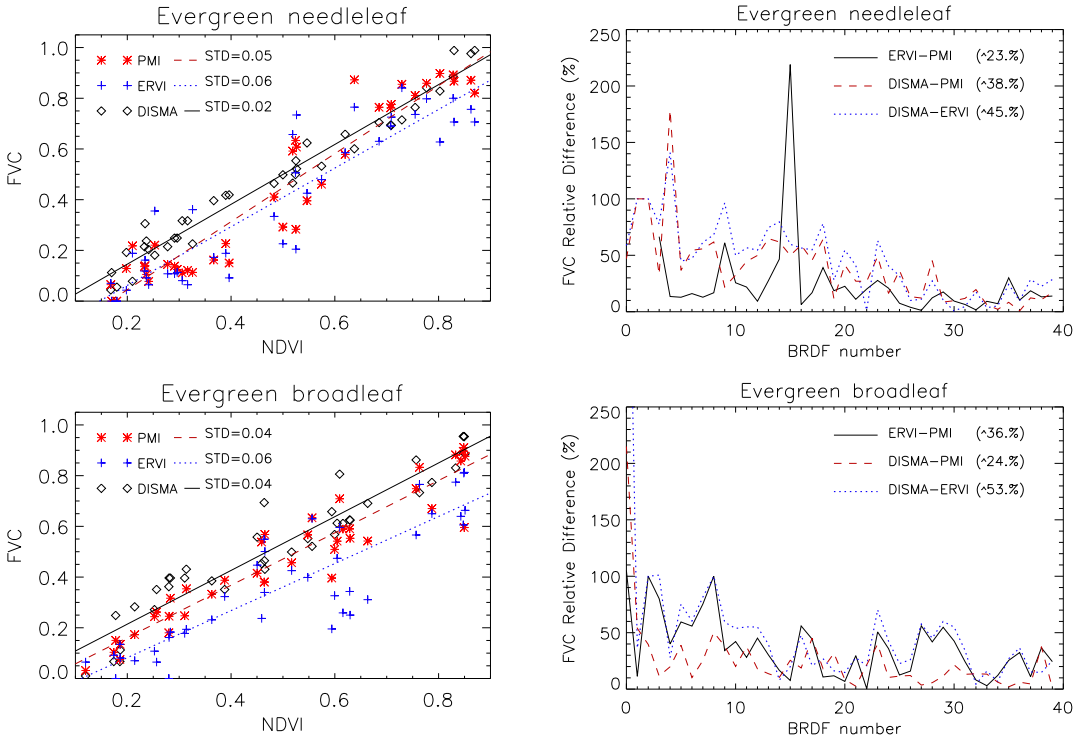

Figure 9.- Retrieved values of LAI using DISMA, PMI, and ERVI approaches (on the left side). FVC relative difference among the different approaches (on the right side)

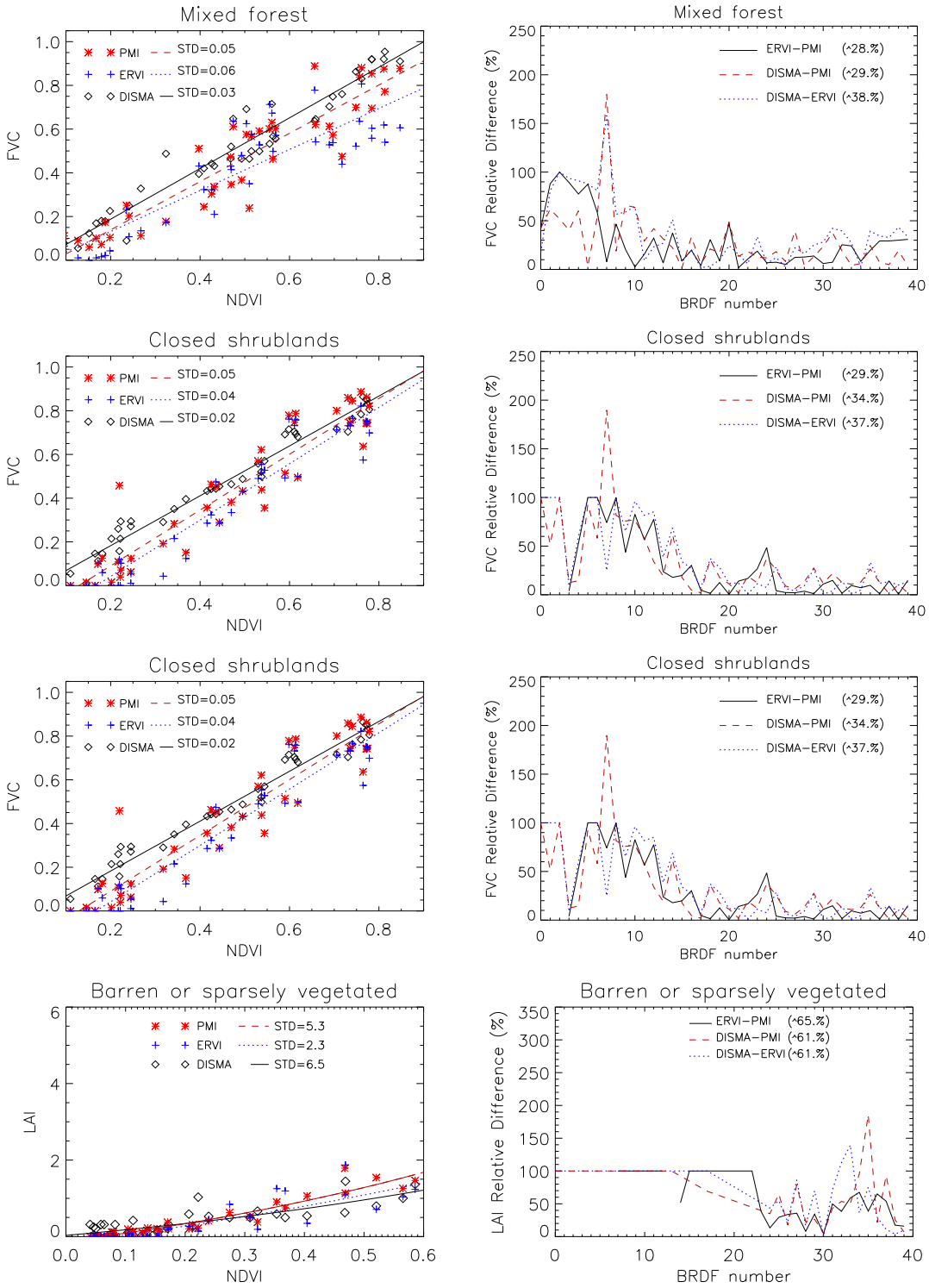

Figure 9.- Continuation

The comparison of the FVC values shows the same increasing linear trend with increasing NDVI, presenting the DISMA outputs slightly lower standard deviations. For all the analysed biomes the ERVI approach provides the lowest FVC estimates, whilst the DISMA approach provides the highest values. The relative difference of DISMA FVC outcomes with the PMI estimates is around 30%, the same relative difference obtained between PMI and ERVI results. The difference between DISMA and ERVI is around 40%.

The DISMA FVC values present a slightly higher dynamic range than the other approaches. The DISMA FVC ranges between 0 and 1 for most of the biomes, with the exception of Closed shrublands where the maximum FVC values is 0.8, and Barren of sparsely vegetation where the maximum value is 0.6, which are in the same level of the POLDER products. The PMI FVC values are only slightly lower than DISMA FVC in most of the analysed IGBP classes. The difference are more important when comparing with the ERVI FVC values, specially in the Mixed Forest where the maximum values of FVC are around 0.6 whereas DISMA and PMI results are close to 0.9. The maximum relative differences are for low NDVI values. The DISMA FVC presents again a bias for bare soil of around 0.1 as it can be seen in the Barren or sparsely vegetation class. This could be produced by a deficient characterization of the soil BRDF. In addition, DISMA produces higher FVC values for NDVI around 0.2 where we must expect very low vegetation coverage. However, DISMA provides FVC close to 30% in most of the cases, and goes beyond in some cases (Savannas). This problem for low vegetation coverage could be solved when applying the overall prototyping algorithm to satellite images. This will be achieved thanks to a more accurate characterization of the soil spectral BRDF and definition of the domain of admitted solutions based in the FVC output of VMESMA module.

5. CONCLUSIONS

During this visiting scientist stay, the DISMA algorithm has been prototyped with monthly synthesis BRDF POLDER/ADEOS data. The feasibility of the DISMA algorithm applied to directional signatures in 3 channels data have been evaluated against standard POLDER products derived from the same input data using two different approaches, empirical relationships with vegetation indices and physical model inversion.

In the prototyping using POLDER/ADEOS data, the Price-Walthall soil model, the clumping index and an automatic method to derive leaf albedo from data have been implemented. Results confirm that the DISMA prototype reproduces accurately the directional signatures of major biomes at coarse spatial resolution. The inversion of the DISMA algorithm provides FVC and LAI estimates, which are physically coherent with the expected according the biome type. For instance, the maximum of the LAI is around 6 for forest (evergreen needleleaf, broadleleaf and mixed forest), close to 4.5 for savannas, to 3 for shrublands and lower than 2 for barren or sparsely vegetation, and similar for the fractional vegetation cover.

The comparison of the DISMA LAI and FVC estimates with the POLDER level 3 Products shows that the estimated vegetation parameters are consistent, showing the feasibility of the DISMA algorithm for retrieving vegetation parameters. In general, the agreement between

DISMA outputs and POLDER products is noticeable. However, the LAI obtained with DISMA underestimate the POLDER LAI values in the range between 0.6-0.8, whereas overestimates the FVC regarding the POLDER products, irrespectively of the amount of vegetation. Nevertheless, the relative differences between DISMA estimates and POLDER vegetation products are not larger than the differences between POLDER products, on the order of 40% for LAI and 30% for FVC, demonstrating the suitability of the DISMA algorithm for retrieving vegetation parameters at coarse spatial resolution.

7. VALUATION AND PROSPECTS

During this stay, the DISMA algorithm has been prototyped to a coarse resolution satellite data. For that, we have taken advantage of the methodologies to derive POLDER vegetation products, for instance to define the soil BRDF model or to incorporate the clumping index estimations in the equations. In addition, an automatic method to retrieve leaf albedo has been tested providing good results. This research has confirmed that the DISMA prototype provide reasonable estimates in the full range of variation of FVC and LAI for biomes of very different architecture. Therefore, the results from the prototyping have constituted a valuable means of testing the underlying physics of the algorithm and also for improving the DISMA algorithm behavior, providing basis for improved retrieval of vegetation parameters from MSG and EPS.

Consequently, the objectives of this visiting scientist stage have been satisfactorily fulfilled. Nevertheless, the results are limited to a small sampling, and several simplifications have been assumed. Once we have demonstrate the suitability of the DISMA algorithm, the next step will be to apply the overall prototyping algorithm over POLDER/ADEOS data to produce FVC and LAI maps, and validate these maps against the POLDER maps on a statistically significance spatial and temporal dimensions.

In addition to that, during this stage several meeting with Météo-France (LSA SAF team) have been undertaken, improving the communication between LSA SAF layers IA y IIID. In particular, this has resulted in several discussions about optimal sampling, validation of the MSG products (Météo-France will participate in the next field campaign at Barrax), and the transfers of data to test our algorithm (Météo-France has provided us a new set of MSG synthetic data along with VEGETATION S1 data). This collaboration results in a strong benefit for us and thus for the good functioning of the LSA SAF project.

Concerning the validation of the MSG vegetation product, it is foreseen to start in July'03 during the intensive field campaign to be carried out at Barrax (SPAIN), with the participation of the ESA (MERIS and CHRIS/PROBA validation) and VALERI project. During this period, the validation of the MSG FVC/LAI in the context of the VALERI project has been defined (during the participation in the VALERI meeting, Avignon, march'03). The Barrax area has been included as test site for VALERI in the 2003. Therefore, VALERI will provide some material and a SPOT image of the area. The field campaign will be coincident with the ESA activities to take full advantage of the manpower along with the ground, airborne and satellite data.

Last but not least, this visiting scientist stage has contributed to establish close links between the Geoland FP6 project and LSA SAF UV team. It is expected that this connection could

serve to improve our strategies for two important forthcoming issues: validation of the MSG products and data fusion (MSG and EPS). It is expected to know the user needs for different communities than meteorological community. For that, it is needed a better knowledge of the users requirements that may translate in an improvement of the LSA SAF product dissemination.

ACKNOWLEDGEMENT

The author thanks to the Visiting Scientist Program of EUMETSAT for founding this research. Special thanks are given to Marc Leroy for supporting this visiting scientist at Médias-France, for several discussions on the prototype and other valuable suggestions. To Roselyne Lacaze and Bastian Miras to provide me all the necessary to carry out this work, and to all the people that I met in Médias-France, especially to Hervé, Fabianne and Chantal for its friendly welcome. To Jean-Louis Roujean and Bernhard Geigher for scientific discussion on the prototype during several meetings in Météo-France. To François-Marie Bréon for discussions on the hot spot issue during my visit at CEA/LSCE. Finally, to my college Javier García-Haro for the implementation of the DISMA model. The BRDF monthly synthesis database has been produced by Médias-France. The original algorithm has been developed by Noveltis (O. Hautecoeur, A. Quesney and T. Lalanne) upon CNES contract. The POLDER data are from CNES/NASDA

REFERENCES

Asrar, G., Kanemasu, E.R., and Yoshida, M. (1985). Estimates of leaf area index from spectral reflectance of wheat under different cultural practices and solar angle. Remote Sensing of Environment, 17:1-11.

Asner, G. P., Bateson, C. A., Privette, J. L., El Saleous, N., and Wessman, C. A., 1998, Estimating vegetation structural effects on carbon uptake using satellite data fusion and inverse modeling. J. Geophys. Res. 103:28,839-28,853.

Baret, F. and G. Guyot, (1991). Potentials and limits of vegetation indices for LAI and APAR assessment. Remote Sensing of Environment, 35: 161-173.

Bicheron, P and M. Leroy, (1999). A Method of Biophysical Parameter Retrieval at Global Scale by Inversion of a Vegetation Reflectance Model. Remote Sensing of Environment, 67: 251-266.

Borel, C.C. and S.A.W. Gerstl, 1994. Nonlinear spectral mixing models for vegetative and soil surfaces, Remote Sens. Environ. 47:403-416.

Camacho de Coca, F., F.J. García-Haro, B. Martínez (2002). An operational strategy for retrieval of vegetation products from SEVIRI & AVHRR-3 data. Proceedings of the LSA SAF Training Workshop, (Ed. EUMETSAT: Darmstadt), Lisboa, 8-10 Julio (in press).

Camacho de Coca, F., F. J. García-Haro, M. A. Gilabert and J. Meliá, (2003) Vegetation cover seasonal changes assessment from TM imagery in a semiarid landscape. International Journal of Remote Sensing (in press).

Chen, J.M. and Leblanc, S.G., 1997, A four-scale bidirectional reflectance model based on canopy architecture. IEEE Trans. Geosci. Remote Sens. 35:1316-1337.

Combal, B., F. Baret, M. Weiss, A. Trubuil, A. Macé, A. Pragnerète, R. Myneni, Y. Knyazikhin and L. Wang, (2002). Retrieval of biophysical variables from bidirectional reflectances using prior information to solve ill-posed inversion problems. Remote Sensing of Environment, 84 : 1-5.

DESCHAMPS, P. Y, BREÓN, F.M., LEROY, M., PODAIRE, A., BRICAUD, A., BURIEZ, J.C. AND SÈZE. G., (1994). The POLDER Mission: Instrument Characteristics and Scientific Objectives. IEEE Transactions on Geoscience and Remote Sensing, vol. 32, nº.3: 598-614.

García-Haro, F.J., F. Camacho de Coca and J.Meliá (2003). Retrieving leaf area index from multi-angular airborne data. Annals of Geophysicae (submitted).

García-Haro F.J., F. Camacho-de Coca and J. Meliá, (2002). Retrieval of biophysical parameters using directional spectral mixture analysis. In Recent advances in quantitative remote sensing, pp. 963-971. J. Sobrino, Ed., Universitat de Valencia.

García-Haro, F.J, Sommer, S. and Kemper, T. (2003b), Variable multiple endmember spectral mixture analysis (VMESMA): a high performance computing and environment analysis tool. International Journal of Remote Sensing (submitted).

Hapke, B., 1981, Bidirectional reflectance spectroscopy: 1. Theory. J. Geophys. Res.86: 3039-3054.

Hapke, B., D. Dimucci, R. Nelson and W.Smythe, (1996). The cause of the hot spot in vegetation canopies and soils: shadow-hiding versus coherent backscatter. Remote Sensing of Environment, 58, 63-68.

Jacquemoud, S. and F. Baret, (1990). PROSPECT: a Model of Leaf Optical Properties Spectra. Remote Sensing of Environment 34:75-91.

Jasinski, M.F. and Eagleson, P.S., (1989). The structure of red-infrared scattergrams of semivegetated landscapes. IEEE Trans. Geosci. Remote Sens. 27: 441-451.

Jasinski, M.F. and Eagleson, P.S., (1990). Estimation of subpixel vegetation cover using red-infrared scattergrams. IEEE Transanctions on Geoscience and Remote Sensing 28: 253-267.

Kemper, T., García-Haro, F.J., Preissler, H., Mehl, W., Sommer, S., (2000), A multiple endmember unmixing approach for mapping heavy metal contamination after the Doñana mining accident (Seville, Spain), Second EARSeL Workshop on Imaging Spectroscopy, Enschede, The Netherlands, 11-13 July 2000.

Knyazikhin, Y., Martonchik, J.V., Myneni, R.B., Diner, D.J. and Running, S.W. (1998). Synergistic algorithm for estimating vegetation canopy leaf area index and fraction of absorbed photosynthetically active radiation from MODIS and MISR data. Journal of Geophysical Research, 103(D24): 32.257-32.275.

Kuusk, A, (1995). A fast, invertible canopy reflectance model, Remote Sensing of Environment, 51:342-350.

Lacaze, R., (2003). POLDER BRDF database. User document. MEDIAS-France Report, 48 pp.

Lacaze, R., (2002). Comparaison des produits LAI POLDER au produit LAI MODIS et aux measures in-situ acquises pendant les campagnes terrain du programme VALERI. MEDIAS-France Report, 82 pp.

Lacaze, R., J.M. Chen, J.L. Roujean, S.G. Leblanc, (2002). Retrieval of vegetation clumping index using hot spot signatures measured by POLDER instrument. Remote Sensing of Environment, 79: 84-95.

Lacaze, R. and Roujean, J.L., (2001), G-function and Hot SpoT (GHOST) reflectance model. Application to multi-scale airborne POLDER measurements. Remote Sens. Environ., 76:67-80.

Leblanc, S.G., P. Bicheron, J .M. Chen, M. Leroy and J. Cihlar, (1997). Investigation of radiative transfer in boreal forest with an improved 4-scale model and airborne POLDER data. IEEE Transactions on Geoscience and Remote Sensing, 27: 1396-1414.

Li, X. and A.H. Strahler, (1992). Geometrical-optical bidirectional reflectance modeling of the discrete crown vegetation canopy: Effect of crown shape and mutual shadowing. IEEE Transactions on Geoscience and Remote Sensing, 24:906-919.

Nilson, T., (1971), A theoretical analysis of the frequency of gaps in plant stands. Agric. Meteorol. 8:25-38.

Nilson, T and A. Kuusk, (1989). A reflectance model for the homogeneous plant canopy and its inversion. Remote Sensing of Environment, 27: 157-167

Price, J.C., (1990). On the information content of soil reflectance spectra. Remote Sensing of Environment, 33: 113-121.

Pinty, B., M. Verstreate and B. Dickinson, (1990). A physical model of the bidirectional reflectance of canopies, 2. Inversion and validation. Journal of Geophysical Research, 95 (D8):11,767-11,775.

Quesney, A., O. Hatecoeur and R. Bru, (2001). Paramétrisation du modèle de Walthall-Price. Optimisation d'un modele de sol nu pour POLDER. NOVELTIS report, 17 pp, NOV-3030-NT-573.

Qin,W. and N.S. Goel, (1995). An evaluation hotspot models for vegetation canopies, Remote Sensing Reviews, 13:121-159.

Qin, W., N.S. Goel and B. Wang, (1996), The hotspot effect in heterogeneous vegetation canopies and performance of various hotspot models, Remote Sensing Reviews, 14, 283-332.

Qin, W. and Gerstl, S.A.W., (2000). 3-D scene modeling of semidesert vegetation cover and its radiation regime, Remote Sens. Environ., 71: 197-206.

Rahman H., Pinty B., Verstraete M.M. (1993), Coupled Surface-Atmosphere Reflectance (CSAR) model. 2. Semi-empirical surface model usable with NOAA Advanced Very High Resolution Radiometer Data, Journal of Geophysical Research, 98: 20791-20801.

Roberts, D. A., Adams, J. B., and Smith, M. O., 1990, Transmission and Scattering of Light by Leaves: the Effect on Spectral Mixtures, Proc. 10th Annual IGARSS, College Park, Md, May 20-24, pp. 1381-1384.

Ross, J.K. (1981). The Radiation Regime and Architecture of Plant Stands. The Hague, Boston, London.

Roujean, J.L. (2000). A parametric hot spot model for optical remote sensing application, Remote Sensing of Environment, 71: 197-206.

Roujean, J. L. and R. Lacaze, (2002). Global mapping of vegetation parameters from POLDER multiangular measurements for studies of surface-atmosphere interactions: A pragmatic method and its validation. Journal of Geophysical Research, 107-D12: ACL6-1-14.

Roujean, J.L. and F.M. Bréon, (1995). Estimating PAR absorbed by vegetation from bidirectional reflectance measurements, 51:373-384.

Roujean, J.L, D.Tanré, F. M. Bréon and J.L. Deuzé, (1997). Retrieval of land surface parameters from airborne POLDER bidirectional reflectance distribution function during HAPEX-Sahel. Journal of Geophysical Research, vol. 102, no. D10: 11,201-11,217.

Van-Leeuwen, W.J.D. and Roujean, J.L. (2002). Land surface albedo from the synergistic use of polar (EPS) and geo-stationary (MSG) observing systems. An assessment of physical uncertainties, Remote Sensing of Environment, 81: 273-289.

Verhoef (1984) Ligth scattering by leaf layers with application to canopy reflectance modeling: the SAIL model. Remote Sensing of Environment 16: 125-141.

Walthall, C.L., J.M. Norman, J.M. Welles, G. Campbell and B.L. Blad, (1985). Simple equation to approximate the bidirectional reflectance from vegetative canopies and bare soil surfaces. Applied Optics, 24: 383-387.

Weiss, M. and F. Baret, (1999). Evaluation of canopy biophysical variable retrieval performances from the accumulation of large swath satellite data. Remote Sensing of Environment, 70: 293-306.

White, H.P., J.R. Miller and J.M. Chen, (2001). Four scale linear model for anisotropic reflectance (FLAIR) for plant canopies-Part I: Model description and partial validation. IEEE Transactions on Geoscience and Remote Sensing, 1072-1083.

Zhang, Y., Y. Tian, Y. Knyazikhin, J.V. Martonchik, D.J. Diner, M. Leroy and R.B. Myneni (2000). Prototyping of MISR LAI and FPAR algorithm with POLDER data over Africa. IEEE Transactions on Geoscience and Remote Sensing, vol. 38, No. 5: 2402-2418.

ANNEX

MEASURED AND MODELLED (DISMA) POLDER SPACEBORNE DIRECTIONAL SIGNATURES OF MAJOR BIOMES

IGBP 01: EVERGREEN NEEDLELEAF FOREST

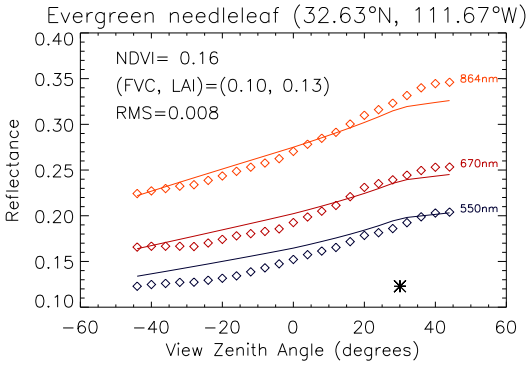

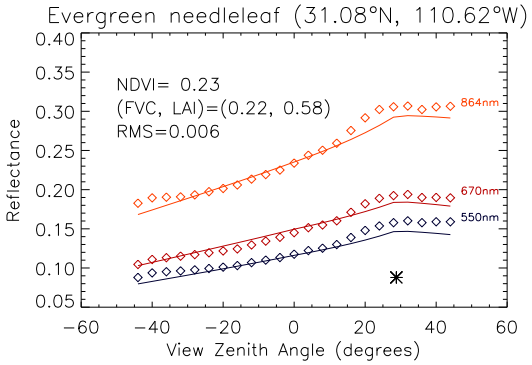

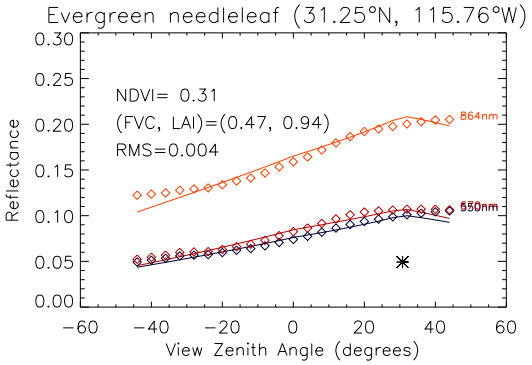

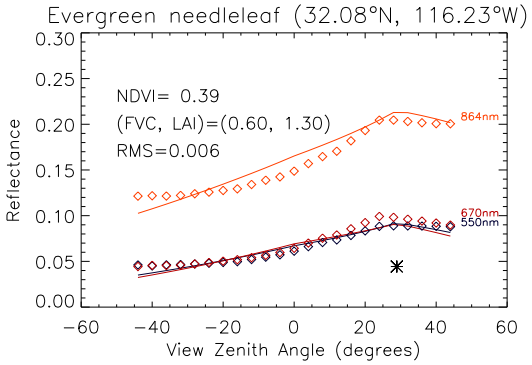

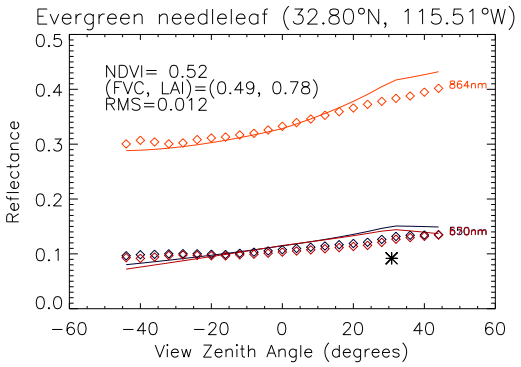

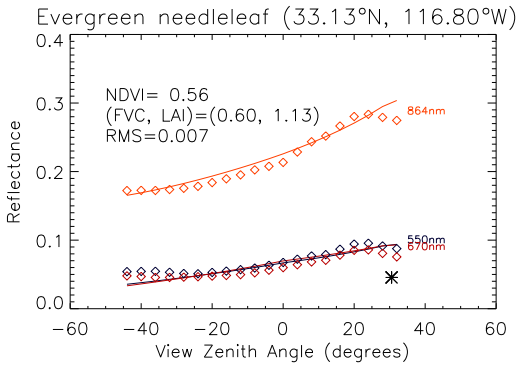

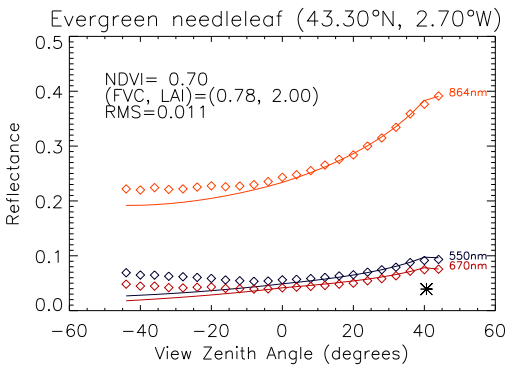

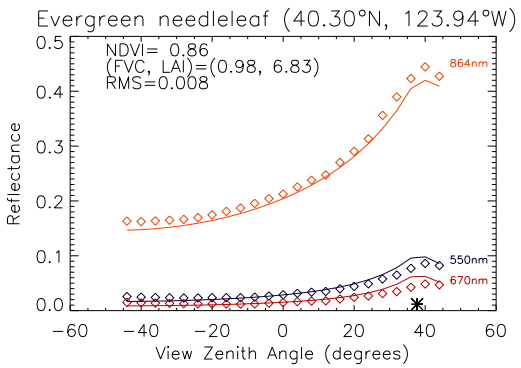

IGBP 02: EVERGREEN BROADLEAF FOREST

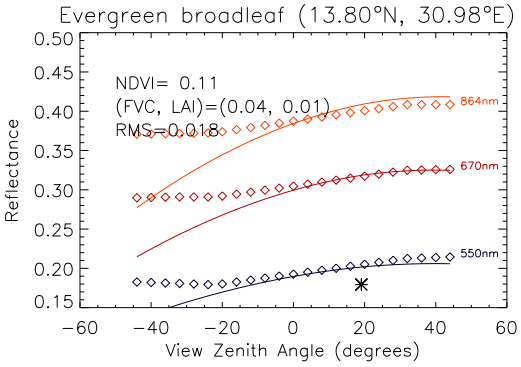

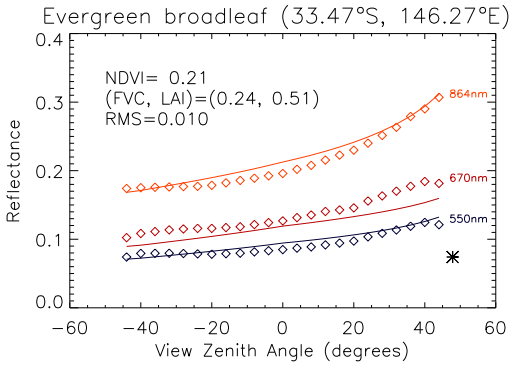

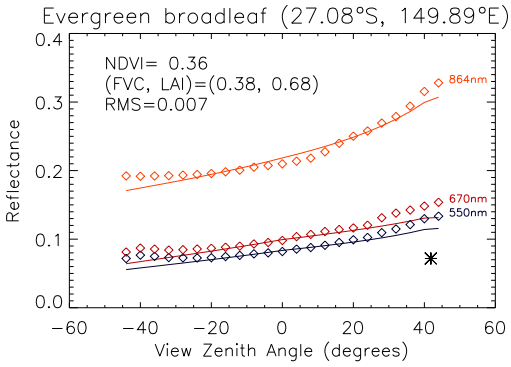

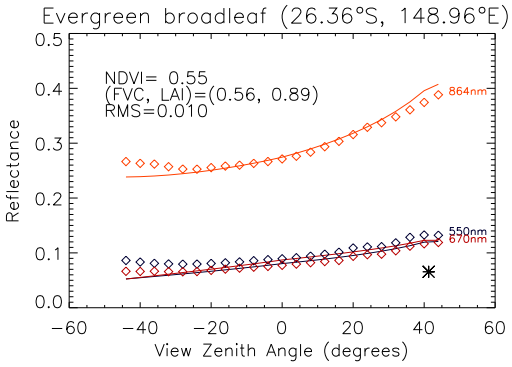

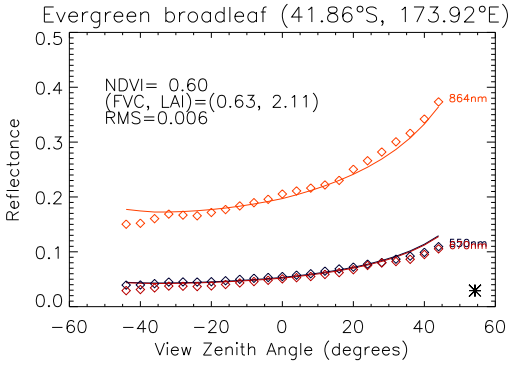

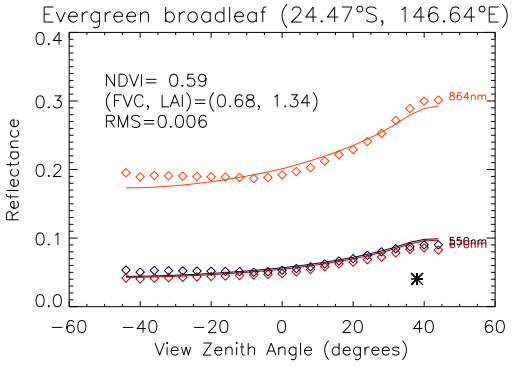

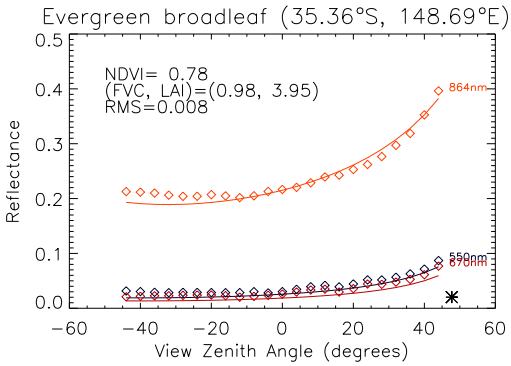

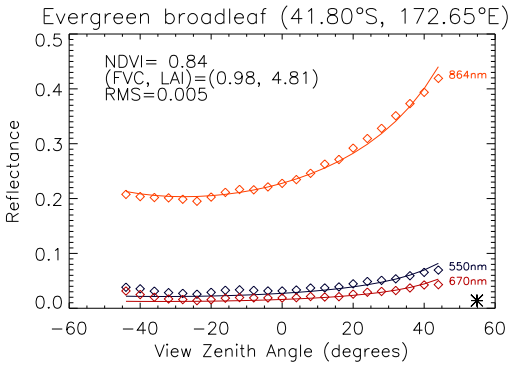

IGBP 05: MIXED FOREST

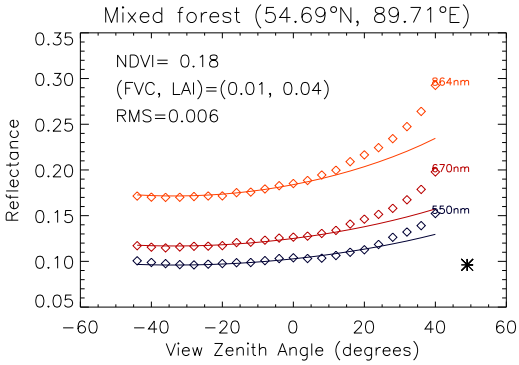

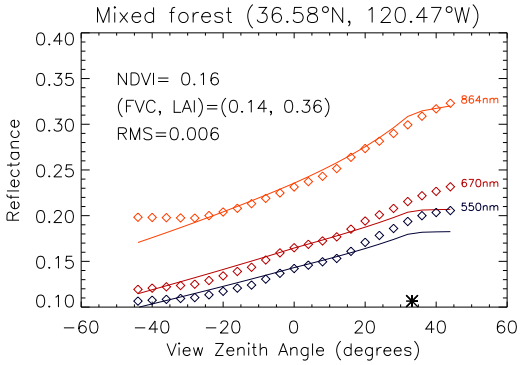

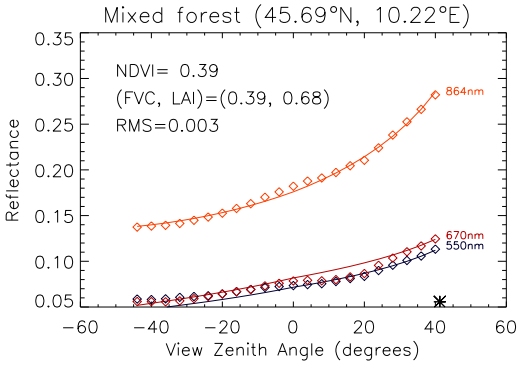

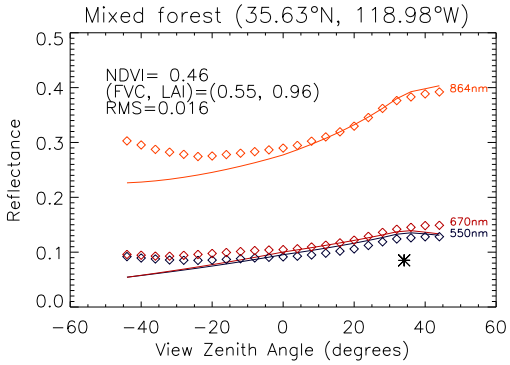

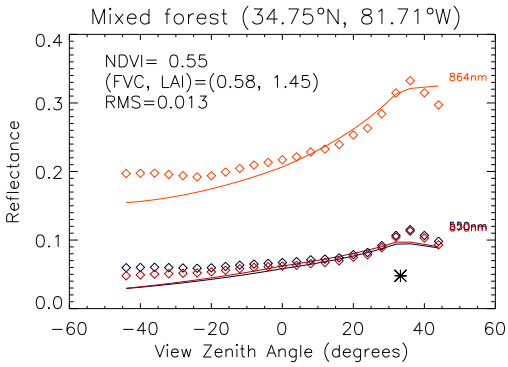

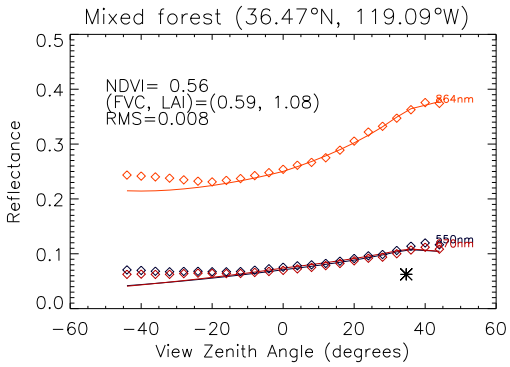

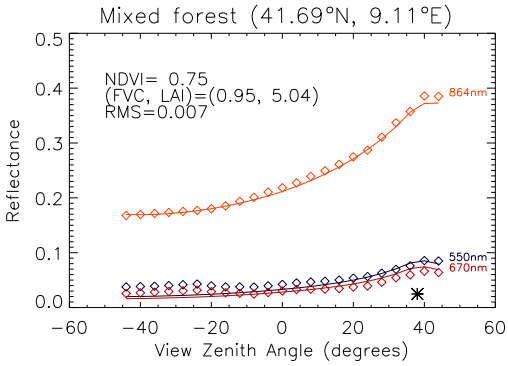

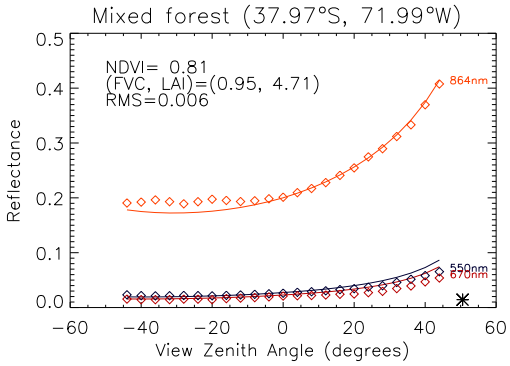

IGBP 06: CLOSED SHRUBLANDS

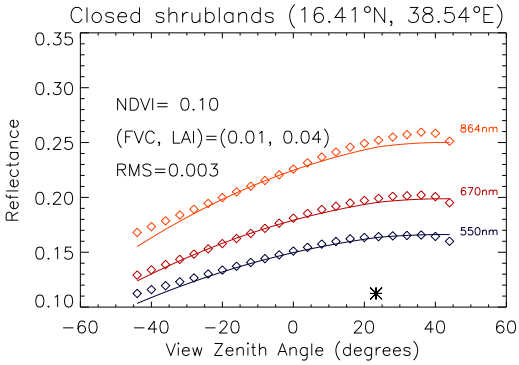

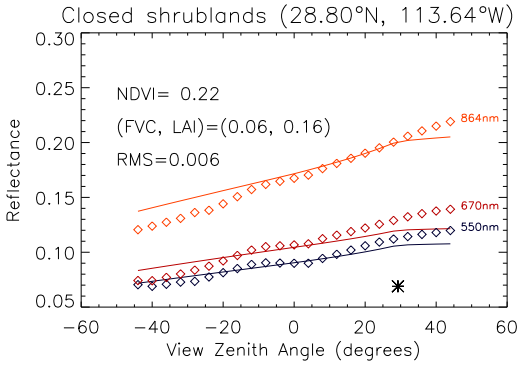

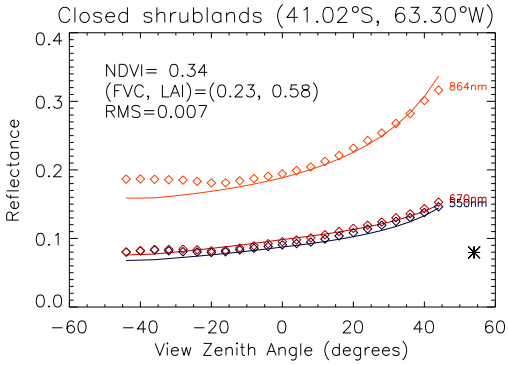

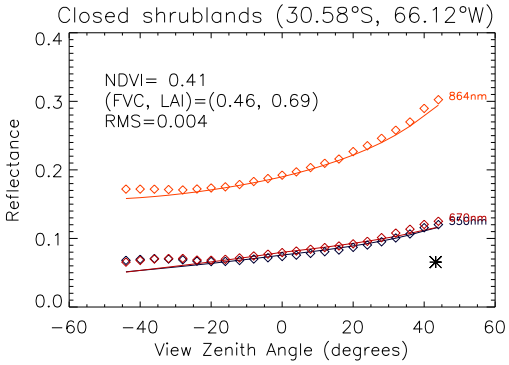

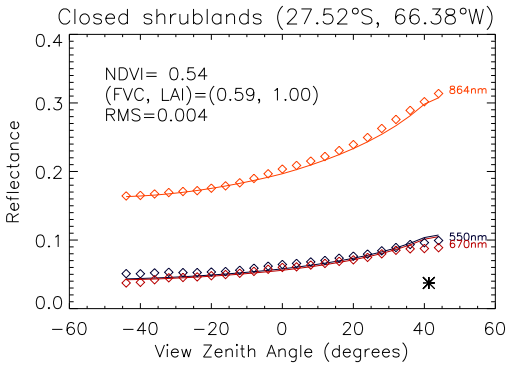

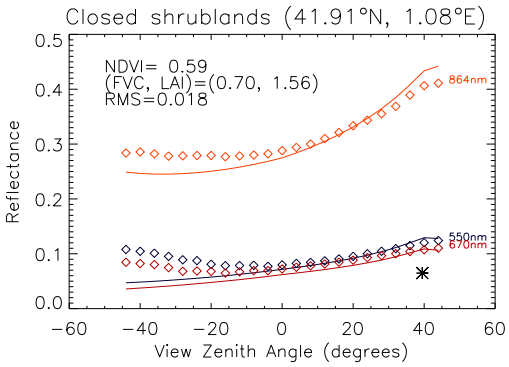

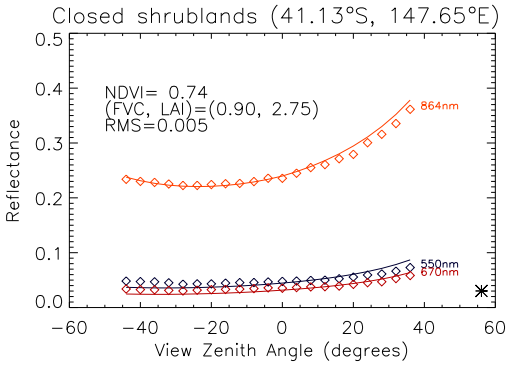

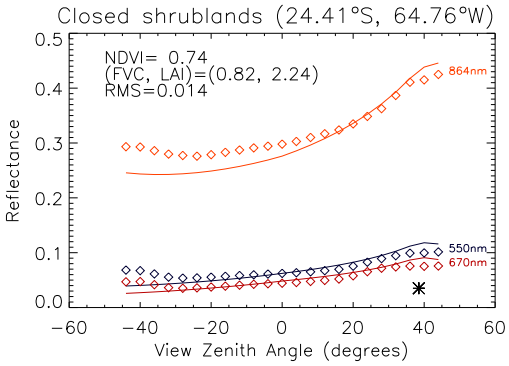

IGBP 09: SAVANNAS

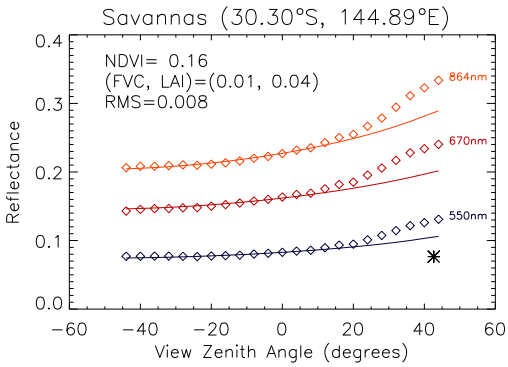

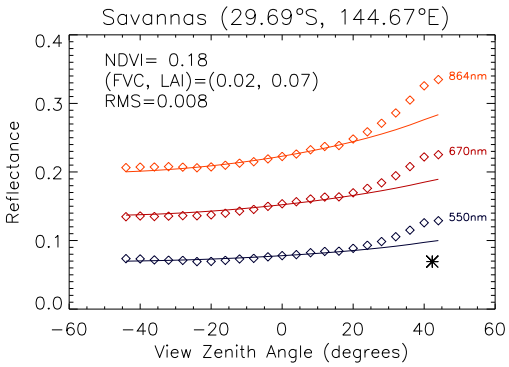

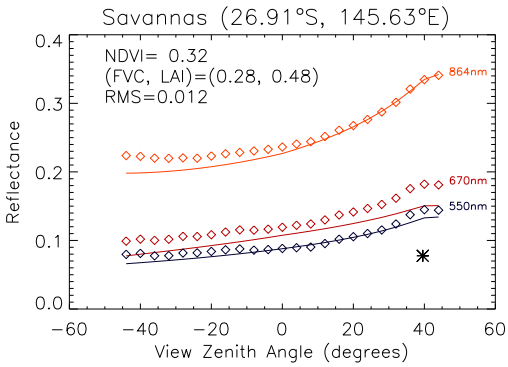

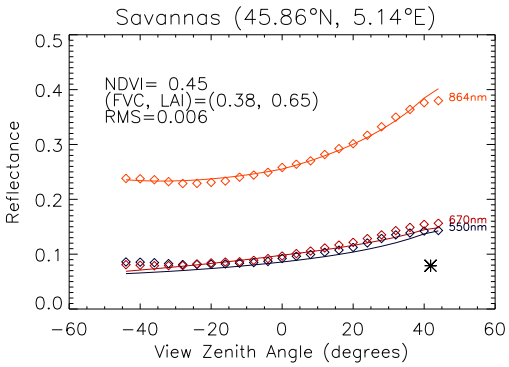

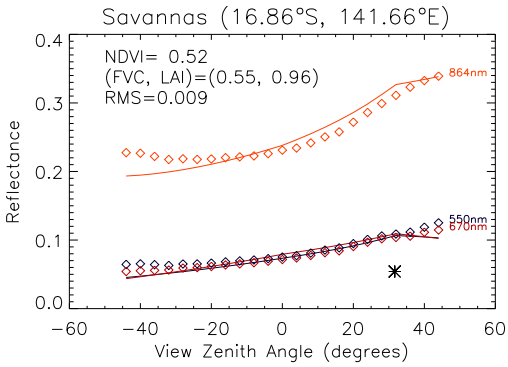

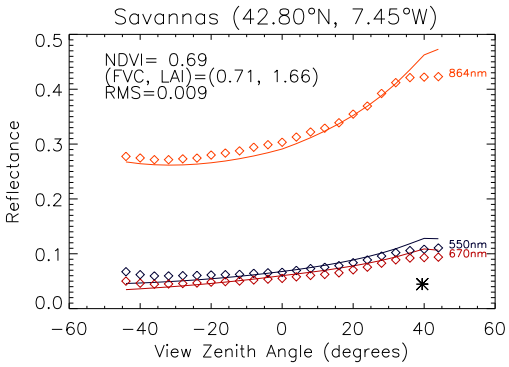

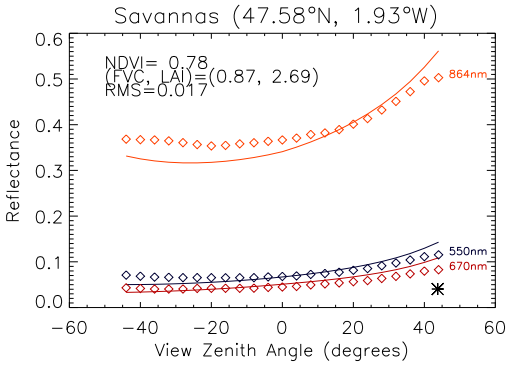

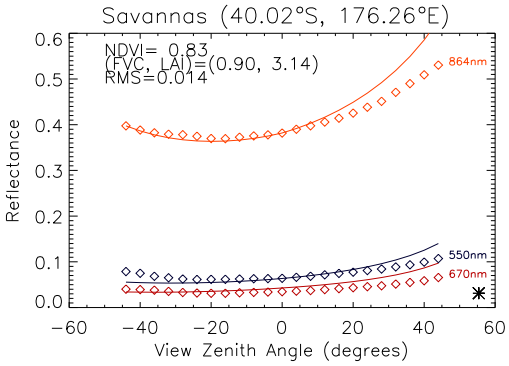

IGBP 09: BARREN OR SPARSELY VEGETATION

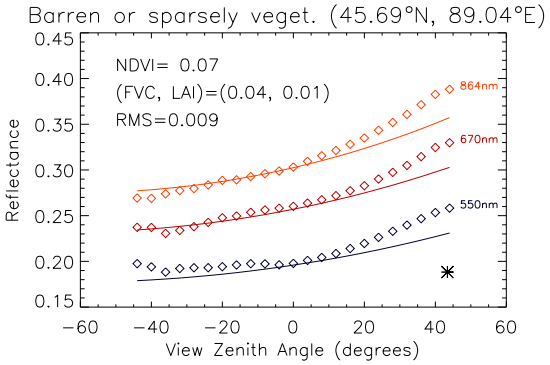

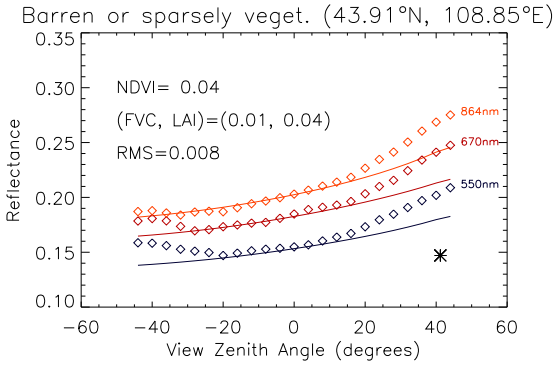

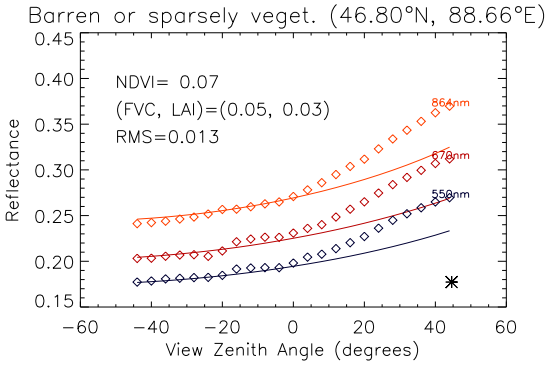

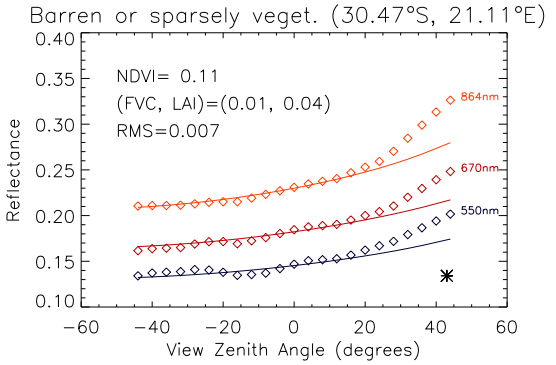

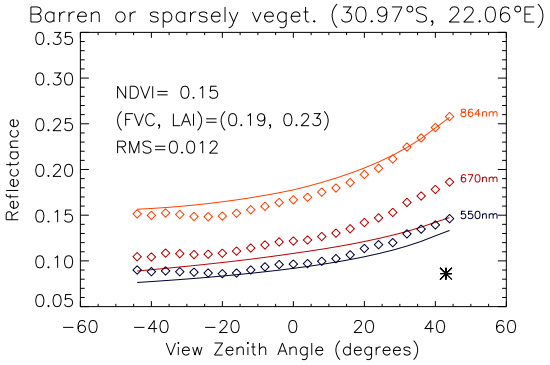

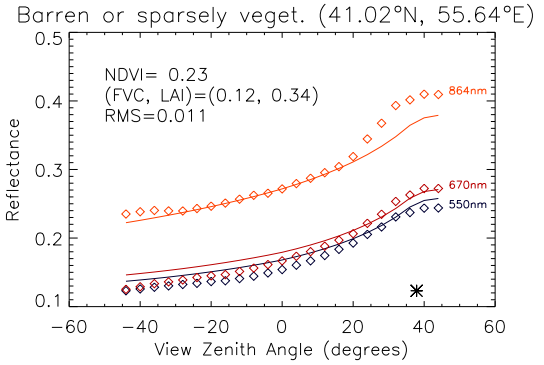

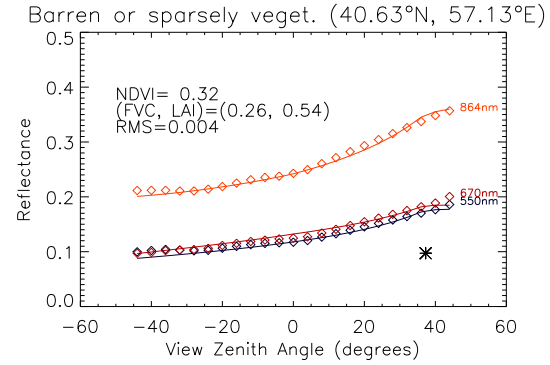

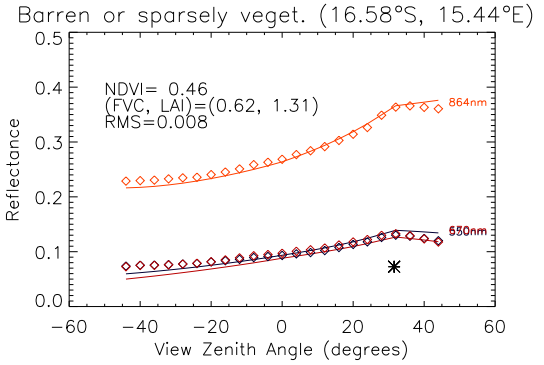

- END -